Journal of Vertebrate Paleontology e1794885 (26 pages)

DOI: 10.1080/02724634.2020.1794885

ARTICLE

SKELETAL ANATOMY OF *ACAENASUCHUS GEOFFREYI* LONG AND MURRY, 1995 (ARCHOSAURIA: PSEUDOSUCHIA) AND ITS IMPLICATIONS FOR THE ORIGIN OF THE AETOSAURIAN CARAPACE

ADAM D. MARSH, *[,1] MATTHEW E. SMITH,[1] WILLIAM G. PARKER, [1] RANDALL B. IRMIS,[2] and BEN T. KLIGMAN [3]

[1]Petrified Forest National Park, Division of Science and Resource Management, Arizona 86028, U.S.A., adam_marsh@nps.gov; matthew_e_smith@nps.gov; william_parker@nps.gov;

[2]Natural History Museum of Utah and Department of Geology & Geophysics, University of Utah, Salt Lake City, Utah 84108-1214, U.S.A., irmis@umnh.utah.edu;

[3]Virginia Tech, Department of Geosciences, Blacksburg, Virginia 24061, U.S.A., benkligman@gmail.com

ABSTRACT—*Acaenasuchus geoffreyi* is a diminutive armored archosaur from the Upper Triassic Chinle Formation of northern Arizona, U.S.A., with uncertain evolutionary relationships and skeletal maturity. Known only from osteoderms, the taxon has been considered a valid taxon of aetosaur, juvenile specimens synonymous with the aetosaur *Desmatosuchus spurensis*, or a non-aetosaurian pseudosuchian archosaur. Here, we describe new fossils of *Acaenasuchus geoffreyi* that represent cranial, vertebral, and appendicular elements as well as previously unknown variations in the dorsal carapace and ventral shield. The skull bones are ornamented with the same anastomosing complex of ridges and grooves found on the paramedian and lateral osteoderms, and the appendicular skeleton resembles that of *Revueltosaurus callenderi*, *Euscolosuchus olseni*, aetosaurs, and other armored archosaurs such as erpetosuchids. Histology of osteoderms from the hypodigm of *Acaenasuchus geoffreyi* shows multiple growth lines, laminar tissue, and low vascularity, evidence that the individuals were close to skeletal maturity and not young juveniles. A revised phylogenetic analysis of early archosaurs recovers *Acaenasuchus geoffreyi* and *Euscolosuchus olseni* as sister taxa and members of a new clade that is the sister taxon of Aetosauria. This new phylogeny depicts a broader distribution of osteoderm character states previously thought to only occur in aetosaurs, demonstrating the danger of using only armor character states in aetosaur taxonomy and phylogeny. *Acaenasuchus geoffreyi* is also a good example of how new fossils can stabilize 'wild card' taxa in phylogenetic analyses and contributes to our understanding of the evolution of the aetosaur carapace.

Citation for this article: Marsh, A. D., M. E. Smith, W. G. Parker, R. B. Irmis, and B. T. Kligman. 2020. Skeletal anatomy of *Acaenasuchus geoffreyi* Long and Murry, 1995 (Archosauria: Pseudosuchia) and its implications for the origin of the aetosaurian carapace. Journal of Vertebrate Paleontology. DOI: 10.1080/02724634.2020.1794885

INTRODUCTION

The Aetosauria are a clade of Late Triassic pseudosuchian archosaurs best known for their interlocking dorsal carapace and ventral shield of osteoderms (Desojo et al., 2013), and as one of the only groups of large-bodied herbivorous tetrapods during the Late Triassic Epoch (Walker, 1961; Small, 2002; Desojo and Vizcaíno, 2009). This diverse group possesses taxonomically informative osteoderms whose abundance in the fossil record has led to them being used for biostratigraphy of Upper Triassic non-marine sedimentary units, especially in the North American Southwest (e.g., the Chinle Formation and Dockum Group), and eastern North America (Newark Supergroup rift basins along Atlantic margin) (see discussions in Long and Murry, 1995; Lucas, 2010; Parker and Martz, 2011; Desojo et al., 2013; Martz and Parker, 2017). Members of this clade include medium-sized to large (>2 m total length; Desojo et al., 2013), wide-bodied taxa (e.g., *Desmatosuchus spurensis*, *Paratypothorax andressorum*, and *Typothorax coccinarum*) and smaller, narrower taxa (e.g., *Aetosaurus ferratus*, *Neoaetosauroides engaeus*, and *Stenomyti huangae*). *Acaenasuchus geoffreyi*, a diminutive taxon named for a small number of aetosaur-like osteoderms from northern Arizona, has been hypothesized to be a small-bodied aetosaur taxon, a juvenile of an existing larger-bodied aetosaur taxon, or a non-aetosaurian pseudosuchian archosaur (Long and Murry, 1995; Heckert and Lucas, 2002a; Parker, 2016a). Here, we redescribe the taxon with new material that includes the first cranial and non-osteoderm postcranial skeletal elements of *Acaenasuchus geoffreyi* and hypothesize its phylogenetic relationships by placing it in an analysis with aetosaurs, closely related taxa, and other early archosaurs.

Charles Camp made a large collection of small vertebrates in 1926 from what he called the "meal pots" (Camp, 1924:756–757) that occur in the upper part of the Blue Mesa Member (sensu Woody, 2003; Martz and Parker, 2010; Martz et al., 2012) of the Chinle Formation in the 'Blue Hills' near St. Johns, Arizona (Fig. 1). The tiny osteoderms in this collection were not described until more specimens were found at the nearby *Placerias* and Downs quarries in the 1980s, and they were first identified as belonging to a juvenile *Desmatosuchus spurensis* (Long and Ballew, 1985). Subsequently, they were named a new taxon of diminutive stagonolepidid aetosaur (Murry and Long, 1989; Long and Murry, 1995), *Acaenasuchus geoffreyi*. Since then, this taxon has again been hypothesized to be a juvenile of *Desmatosuchus spurensis* (Lucas and Heckert, 1996a, 1996b; Estep et al., 1998, Heckert and Lucas, 1999, 2000, 2002a), a

*Corresponding author.

Color versions of one or more of the figures in the article can be found online at www.tandfonline.com/ujvp.

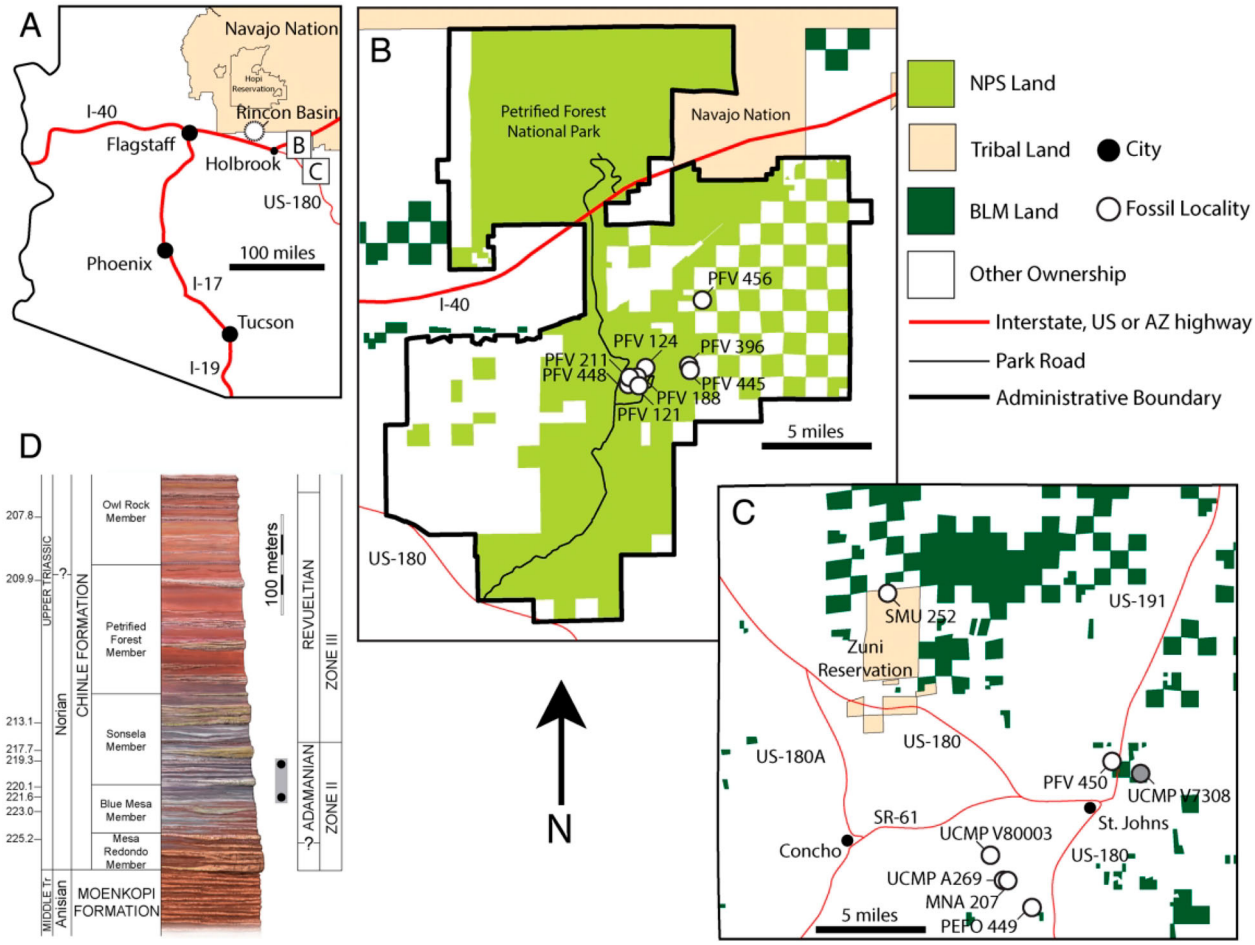

FIGURE 1. Localities from where *Acaenasuchus geoffreyi* is known in **A**, Arizona, U.S.A., **B**, at Petrified Forest National Park, **C**, near St. Johns, and their **D**, stratigraphic distribution. The shaded circle in **C** for UCMP V7308 represents the holotype locality and the dashed circle in **A** for Rincon Basin E represents the lost specimen mentioned in Long and Murry (1995). U-Pb detrital zircon dates modified from Ramezani et al. (2011, 2014) and Atchley et al. (2013).

valid small-bodied aetosaur taxon different from *Desmatosuchus spurensis* (Hunt, 1998; Hunt and Wright, 1999; Irmis, 2005; Parker, 2005a, 2005b; Desojo et al., 2013), a possible sister taxon of *Desmatosuchus spurensis* (Harris et al., 2003; Kischlat, 2000), or perhaps not even an aetosaur at all (Parker, 2008, 2016a). *Acaenasuchus geoffreyi* is not always included in anatomical phylogenetic analyses owing to its highly incomplete nature (e.g., Parker, 2016a), but when it is included it is usually recovered as a member of the stagonolepidid sub-clade Desmatosuchinae (Parker, 2007; Desojo et al., 2012; Heckert et al., 2015; Schoch and Desojo, 2016).

Anatomical modules or regions (e.g., the pectoral girdle and forelimb, the skull, the carapace, etc.) may evolve at different rates in different groups (Thompson, 1917; de Beer, 1954; Takhtajan, 1991; Rae, 1999; Clarke and Middleton, 2008; Mounce, 2013; Parker, 2016a), so taxa named for incomplete specimens that are only represented by one module often act as wild card taxa in phylogenetic analyses (Donoghue et al., 1989; Kearney, 2002; Kearney and Clark, 2003; Norell and Wheeler, 2003). Furthermore, juvenile specimens can also be recovered in phylogenetic positions different from those of adults of the same species (e.g., Fink, 1981; Tykoski, 2005; Wiens et al., 2005; Campione et al., 2013; Tsai and Fordyce, 2014; Griffin, 2018; Gee, 2020). The taxonomic and ontogenetic uncertainty surrounding *Acaenasuchus geoffreyi* is compounded by these problems. Here, we describe new fossils representing cranial, vertebral, and appendicular elements of *Acaenasuchus geoffreyi*, as well as additional osteoderms that preserve carapace variation in the taxon and re-evaluate the original hypodigm. We also perform osteohistological analysis to assess skeletal maturity of specimens belonging to the hypodigm and use this new information in a revised phylogenetic analysis of early archosaurs.

Institutional Abbreviations—**AMNH**, American Museum of Natural History, New York, New York, U.S.A.; **CRILAR**, Centro Regional de Investigaciones Científicas y Transferencia Tecnológica de La Rioja, La Rioja, Argentina; **DMNH**, Denver Museum of Nature and Science, Denver, Colorado, U.S.A.; **ELGNM**, Elgin Museum, Elgin, Scotland, U.K.; **MCP**, Museo de Ciencias e Tecnología, Porto Elegre, Brazil; **MCZ**, Museum of Comparative Zoology, Harvard University, Cambridge, Massachusetts, U.S.A.; **MDM**, Mesalands Dinosaur Museum and Natural Sciences Laboratory, Mesalands Community College, Tucumcari, New Mexico, U.S.A.; **MMACR**, Museu Municipal Aristides Carlos Rodrigues, Candelária, Brazil; **MNA**, Museum of Northern Arizona, Flagstaff, Arizona, U.S.A.; **NCSM**, North Carolina State Museum, Raleigh, North Carolina, U.S.A.; **NHMUK PV R**, Natural History Museum, London, England, U.K.; **NMMNH**, New Mexico Museum of Natural History and

Science, Albuquerque, New Mexico, U.S.A.; **NMT**, National Museum of Tanzania, Dar es Salaam, Tanzania; **PEFO**, Petrified Forest National Park, Arizona, U.S.A. (PFV refers to a locality number from PEFO); **PVL**, Paleontología de Vertebrados, Instituto 'Miguel Lillo,' San Miguel de Tucumán, Argentina; **SMNS**, Staatliches Museum für Naturkunde, Stuttgart, Germany; **SMU**, Shuler Museum of Paleontology, Southern Methodist University, Dallas, Texas, U.S.A.; **SNSB-BSPG**, Staatliche Naturwissenschaftliche Sammlungen Bayerns, Bayerische Staatssammlung für Paläontologie und historische Geologie, München, Germany; **TMM**, Texas Vertebrate Paleontology Collections, the University of Texas at Austin, Austin, Texas, U.S.A.; **TTU-P**, Museum of Texas Tech University, Lubbock, Texas, U.S.A.; **UCMP**, University of California Museum of Paleontology, Berkeley, California, U.S.A.; **UCM**, The University of Colorado Museum, Boulder, CO, U.S.A.; **UMMP**, University of Michigan Museum of Paleontology, Ann Arbor, Michigan, U.S.A.; **UMNH**, Natural History Museum of Utah, Salt Lake City, Utah, U.S.A.; **USNM**, National Museum of Natural History, Smithsonian Institution, Washington, D.C., U.S.A.; **UWBM**, Burke Museum of Natural History and Culture, University of Washington, Seattle, Washington, U.S.A.; **YPM**, Yale Peabody Museum of Natural History, Yale University, New Haven, Connecticut, U.S.A.; **ZPAL**, Institute of Paleobiology of the Polish Academy of Sciences, Warsaw, Poland.

MATERIALS AND METHODS

Mesalands Community College collected vertebrate fossils from PEFO in 1996 and 1998 that were later kept at the New Mexico Museum of Natural History. These fossils were returned to the park in 2013 and included uncatalogued specimens of *Acaenasuchus geoffreyi* but lacked any locality data other than the name 'Dinosaur Ridge' and sub-locality numbers from a general area in the Blue Forest (PFV 211; Hunt, 1998; Hunt and Wright, 1999). We visited the general area in 2001 and 2002 but did not notice any bones of *Acaenasuchus geoffreyi* on the surface at that time.

The 2014 PEFO field crew returned to the Dinosaur Ridge area and found fossils of *Acaenasuchus geoffreyi* nearby at PFV 448 but not at PFV 211 proper (Fig. 1). Preparators tried to find fits between the 2014 material and the 1998 material but were unsuccessful. In 2016, the PEFO field crew returned and rediscovered the remains of the original pin flags that marked the 1998 MDM sub-localities of PFV 211 and found abundant *Acaenasuchus geoffreyi* skeletal elements. When these new collections were reunited with the 1998 collections, preparators immediately found fits and were able to combine the collections and reconstruct osteoderms and portions of vertebrae (Fig. 2E). Additional screen-washing of matrix from PFV 211 produced fragments, some less than 3 mm in size, which allowed preparators to find fits with 1998 material and associate particular collections that only had generic 'Dinosaur Ridge' locality information with specific sub-localities.

The 2016 excavations made it clear that the surface collections made by Mesalands Community College and their volunteers in the general vicinity of Dinosaur Ridge contained relatively fewer bones of *Acaenasuchus geoffreyi* compared to their specific sub-localities (MDM 392, MDM 395, and MDM 399) that were rich in *Acaenasuchus geoffreyi*. The sub-localities represent the remnants of erosive pipes (e.g., Carroll, 1949; Jones, 1971; Barendregt and Ongley, 1977) that when screen-washed contained primarily cranial and post-cranial skeletal material from *Acaenasuchus geoffreyi*, osteoderms of *Vancleavea campi*, and various small reptile vertebrae. Other fossils found among the PFV 211 sub-localities include coprolites, actinopterygian scales, temnospondyl fragments, phytosaur teeth, pieces of large aetosaur osteoderms, and a crocodylomorph osteoderm, but these are far less common than osteoderms of *Acaenasuchus geoffreyi* and *Vancleavea campi*. Because the skeletal anatomy of *Vancleavea campi* is well known (Long and Murry, 1995; Parker and Barton, 2008; Nesbitt et al., 2009), we can easily distinguish its elements from those of *Acaenasuchus geoffreyi*.

Preparation of PEFO fossils of *Acaenasuchus geoffreyi* included adhering small fragments with a 1:2 solution (by volume) of Paraloid B-72 in acetone. All work on PEFO specimens was done under a Leica MZ6 binocular microscope with 10× oculars and a 1.0× objective at up to 40× magnification, or a Wild M7A with 10× oculars and a 1× objective at up to 30× magnification. Minimal matrix removal was performed with water on a soft bristled brush or with a 1/32-inch chisel-pointed carbide needle in a pin vise. In addition, minimal air abrasion was performed on some specimens with a Crystal Mark Swam-blaster MV-1 using iron powder screened through a 0.0025 inch, Tyler equivalent 250 mesh screen. The abrasion was done between 1 and 6 psi with a flow of 1–2 set on the dial. The air abrasion was performed under a Wild M65S surgical scope with 10× objectives and f = 200 mm objective at up to 25× magnification. We molded and cast certain PEFO specimens to reconstruct a vertebra; molds were made with Polytek Platsil 73-25 silicone rubber and casts were made with Polytek EasyFlo 60 polyurethane.

UCMP specimens from the holotype locality UCMP V7308 were initially prepared sometime between collection in the 1930s and publication in 1995. Select UCMP specimens were further prepared for this study using the same equipment and materials as applied to the PEFO specimens. Some of the elements from this locality displayed fresh breaks from collection or damage during storage, but also sometimes a curious weathering pattern that suggested that the material was pre-depositionally eroded or weathered along existing breaks. A good example of this is observed on the anterior bar of the holotype specimen (Fig. 2A). Numerous needle marks were evident on the specimens from earlier attempts at preparation. In addition, various unknown adhesives and surface coatings had to be removed or modified because they obscured much of the surface anatomy. Most of the historic adhesive was relatively clear and readily soluble in acetone and smelled like a cellulose nitrate adhesive such as Devcon (previously DuPont) Duco Cement. The yellowing surface consolidant may have been a type of shellac; it was only moderately soluble in ethanol. Both of these adhesives may have been applied soon after collection, as they were commonly used for contemporary paleontological preparation (Camp and Hanna, 1937). Under the shellac, the bone had softened significantly and was very easily scratched. A ca. 5% solution of Butvar B-76 in acetone was diluted again by half and used to consolidate the bone surface before the chisel-tipped needle was used to physically thin the shellac until it could be lifted away. The bone was relatively hard and firm under the needle in areas where no historic surface consolidants had been applied. In some cases, the remaining matrix released easily from the uncoated bone. In other cases, ferrous minerals or clays remained on the surface and little surface preparation occurred in order to not damage the specimen. We did not prepare any of the previously collected MNA or SMU specimens. UMNH specimens were surface collected by the Utah Geological Survey and were not mechanically prepared or treated with any consolidants.

Two osteoderm specimens (UCMP 175103 and UCMP 175114) from the type locality were selected for osteohistological analysis. The bones were photographed, molded using silicone rubber, and cast in epoxy resin prior to sectioning. Histological sampling and slide preparation were conducted at UCMP and followed the methods of Lamm (2013). Both bones were vacuum-embedded in US Composites Silmar-41 clear polyester resin and allowed to cure for at least 72 hours. 1–1.5 mm-thick sections were cut using a Buehler IsoMet 1000 saw and were affixed to

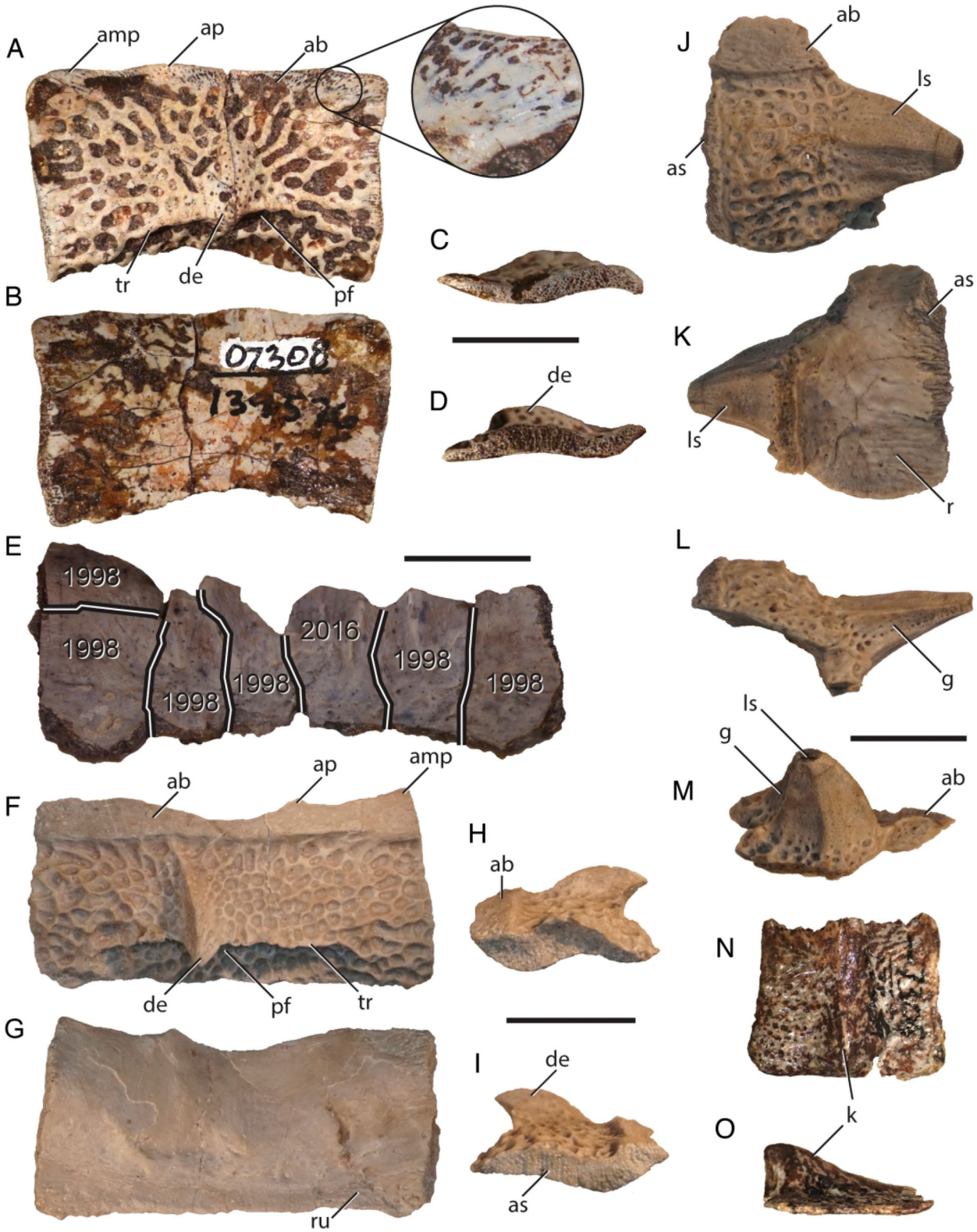

FIGURE 2. *Acaenasuchus geoffreyi*, osteoderms. **A**–**D**, UCMP 139576, holotype right paramedian osteoderm in **A**, dorsal, **B**, ventral, **C**, right lateral, and **D**, left lateral views. **E**, PEFO 40694, right paramedian osteoderm in ventral view. **F**–**I**, PEFO 40000, left paramedian osteoderm in **F**, dorsal, **G**, ventral, **H**, left lateral, and **I**, right lateral views. **J**–**M**, PEFO 40741, right lateral osteoderm in **J**, dorsal, **K**, ventral, **L**, posterior, and **M**, right lateral views. **N**, **O**, UCMP 175139, ventral osteoderm in **N**, ventral and **O**, right lateral views. Inset in **A** is magnified 10×. **Abbreviations**: **ab**, anterior bar; **amp**, anteromedial projection; **ap**, anterior projection; **as**, articulating surface; **de**, dorsal eminence; **g**, groove; **k**, keel; **ls**, lateral spike; **pf**, posterior fossa; **tr**, transverse ridge. Scale bars equal 1 cm.

petrographic glass slides using two-part two-ton epoxy. Using progressively finer grit sizes, the sections were ground with silicon carbide papers on a Buehler Ecomet 3 grinder-polisher. UCMP 175103, a paramedian osteoderm, was longitudinally sectioned along an anterior–posterior axis through the dorsal eminence. UCMP 175114, a lateral osteoderm, was sectioned both longitudinally through the anterior–posterior axis of the main body of the element, and transversely through the lateral spike. The completed histological slides were imaged in plane and cross-polarized light using a Zeiss Axio Imager.M2m petrographic microscope with accompanying Zen 2 v2.0.0.0 software at the University of Utah.

SYSTEMATIC PALEONTOLOGY

ARCHOSAURIA Cope, 1869 sensu Sereno, 2005
PSEUDOSUCHIA von Zittel, 1887 sensu Sereno, 2005
SUCHIA Krebs, 1974 sensu Nesbitt, 2011
ACAENASUCHUS GEOFFREYI Long and Murry, 1995

Desmatosuchus haplocerus Long and Ballew, 1985:61 (juvenile).
"*Acaenasuchus geoffreyi*" Murry and Long, 1989:33 (nomen nudum).
Desmatosuchus haplocerus Lucas and Heckert, 1996a:60 (juvenile aetosaur).
Desmatosuchus haplocerus Lucas and Heckert, 1996b:75 (juvenile aetosaur).
Desmatosuchus haplocerus Estep et al., 1998:40a (juvenile aetosaur).
Acaenasuchus geoffreyi Hunt, 1998:136 (aetosaur).
Desmatosuchus haplocerus Heckert and Lucas, 1999:62 (juvenile aetosaur).
Acaenasuchus geoffreyi Hunt and Wright, 1999:100 (aetosaur).
Desmatosuchus haplocerus Heckert and Lucas, 2000:1561 (juvenile aetosaur).
Acaenasuchus geoffreyi Kischlat, 2000:288 (aetosaur).
Desmatosuchus haplocerus Heckert and Lucas, 2002a:206 (juvenile aetosaur).
Acaenasuchus geoffreyi Harris et al., 2003:242 (desmatosuchine aetosaur).
Acaenasuchus geoffreyi Irmis, 2005:75 (aetosaur).
Acaenasuchus geoffreyi Parker, 2005a:38 (stagonolepidid aetosaur).
Acaenasuchus geoffreyi Parker, 2005b:331 (aetosaur).
Acaenasuchus geoffreyi Parker, 2007:16 (desmatosuchine aetosaur).
Acaenasuchus geoffreyi Parker, 2008:37 (aetosaur).
Acaenasuchus geoffreyi Desojo et al., 2013:206 (aetosaur).
Acaenasuchus geoffreyi Desojo et al., 2012:27 (desmatosuchine aetosaur).
Acaenasuchus geoffreyi Heckert et al., 2015:10 (desmatosuchine aetosaur).
Acaenasuchus geoffreyi Schoch and Desojo, 2016:88 (desmatosuchine aetosaur).
Acaenasuchus geoffreyi Parker, 2016a:6 (non-aetosaurian pseudosuchian).

Holotype—UCMP 139576, right paramedian osteoderm (Fig. 2A–D).

Referred Specimens—Incomplete lists of specimens referred to *Acaenasuchus geoffreyi* are found elsewhere (Long and Murry, 1995; Heckert and Lucas, 2002a; Polcyn et al., 2002), and a complete list of specimens is found in Appendix 1 and more detailed information is found in Supplementary Data 1. Surface files of selected PEFO specimens are available in Supplementary Data 2 at www.morphobank.org (MorphoBank project P3406). All referred specimens from PEFO, MNA, and UCMP were observed first-hand.

Removed Specimens—The following specimens have been referred to *Acaenasuchus geoffreyi* (pp. 212–213 in Heckert and Lucas, 2002a), but either lack the character states that diagnose the taxon (see below) or are lost. When appropriate, we provide re-identification of these elements in parentheses. UCMP 27049 (Metoposauridae); UCMP 175104, UCMP 175136, UCMP 175140, UCMP 175140, UCMP 175142, and UCMP 175143 (*Revueltosaurus* sp.); UCMP 139584, UCMP 139584, UCMP 139585, UCMP 156046, and UCMP 175121 (lost); the UCMP Rincon Basin E specimens (Long and Ballew, 1985; Long and Murry, 1995) may be two uncatalogued osteoderm fragments from a mis-routed loan at the MNA that are in a box labeled 'Tovar Mesa, Winslow.'

Revised Diagnosis—*Acaenasuchus geoffreyi* can be distinguished from all other pseudosuchian archosaurs by the following autapomorphies: small horn present on the posterior process of the squamosal (Fig. 3E); transverse process of trunk vertebrae ornamented distally (Fig. 3M); rounded tubercle present on the lateral surface of the ilium between the preacetabular process and supraacetabular crest (Fig. 4H); dorsal eminence of the paramedian osteoderms forms a "thorn-like process" (Long and Murry, 1995:114; Fig. 2F) or posteriorly curved spike; triangular boss of lateral osteoderm forms a posteriorly curved spike (Fig. 2J); and presence of external lateral osteoderms (an osteoderm ventrolateral to the 'internal' lateral osteoderm but dorsal to the ventral osteoderms (Fig. 5H, L). *Acaenasuchus* can further be distinguished by the following unique combination of character states: anterior edge of anterior margin of some paramedian osteoderms is straight (shared with *Longosuchus meadei*, *Lucasuchus hunti*, *Sierritasuchus macalpini*, and *Desmatosuchus*), dorsal eminence of paramedian osteoderms does not contact posterior margin of the osteoderm in most rows (shared with *Desmatosuchus spurensis*), lateral osteoderms in cervical region have a slightly recurved spine rather than an elongated horn like those of *Desmatosuchus spurensis* and some typothoracines (shared with *Lucasuchus hunti*).

Locality and Horizon—The holotype specimen UCMP 139576 and many referred specimens were collected from UCMP V7308, St. Johns 2 (= 'Blue Hills 1' of Long and Murry, 1995; field number CLC 36/8) a few miles northeast of the city of St. Johns in Apache County, Arizona (Fig. 1B). UCMP V7308 occurs in the upper part of the Blue Mesa Member of the Upper Triassic Chinle Formation (sensu Woody, 2003; Irmis, 2005; Parker, 2005a, 2018a). *Acaenasuchus geoffreyi* also occurs in the upper Blue Mesa Member near St. Johns, Arizona at PFV 449 (Salado Site; Ramezani et al., 2014), PFV 450 (US 191 Site), and SMU 252 (Stinking Springs; Polcyn et al., 2002). The taxon is found in the upper part of the Blue Mesa Member at eight localities in Petrified Forest National Park (Fig. 1A): PFV 121 (Phytosaur Basin E; field number CVB 18/72), PFV 124 (Blue Mesa E), PFV 188 (Dying Grounds Microvertebrate Locality; Heckert, 2004), PFV 396 (Coprolite Layer; Kligman et al., 2017, 2018), PFV 445 (*Doswellia* Quarry), PFV 456 (Thunderstorm Ridge), and PFV 211 (Dinosaur Ridge; Hunt, 1998), which is split into several sub-localities (MDM 392, 395, and 399). *Acaenasuchus geoffreyi* is also found in the lower part of the Sonsela Member at UCMP A269 (*Placerias* Quarry; Fig. 1B), UCMP V80003 (Camp's 'Old' A269), and MNA 207 (Downs Quarry), which is laterally equivalent to the *Placerias* Quarry (Jacobs and Murry, 1980; Kaye and Padian, 1994). Long and Murry (1995) mention a paramedian plate that was shown to Robert Long by Gordon Nelson from an unknown locality north of Winslow, Arizona near Tovar Mesa (Rincon Basin E; Fig. 1), but the specimen was thought to be in a private collection (see above) and Long's field notes do not elaborate on the locality (pp. 159–160 of Robert Long field notes, 1982; Long and Ballew, 1985). As discussed below, a

FIGURE 3. *Acaenasuchus geoffreyi*, axial elements. **A**, **B**, UCMP 285854, left frontal in **A**, dorsal and **B**, ventral views. **C**, **D**, UCMP 285909, left parietal in **C**, dorsal and **D**, ventral views. **E**, **F**, UCMP 156046, left squamosal in **E**, dorsal and **F**, ventral views. **G**, **H**, UCMP 285909, jugal in **G**, lateral and **H**, medial views. **I**, **J**, PEFO 43699, left maxilla in **I**, lateral and **J**, medial views. **K**, **L**, UCMP 293853, left articular and surangular in **K**, lateral and **L**, dorsal views. **M**–**P**, PEFO 40687, trunk vertebra in **M**, dorsal, **N**, ventral, **O**, anterior, and **P**, posterior views. **Q**, **R**, UCMP 175117, trunk vertebra in **Q**, right lateral and **R**, anterior views. **S**, **T**, UCMP 192558, cast of trunk vertebra in **S**, dorsal and **T**, ventral views. **U**, **V**, UCMP 192558, sacral vertebra in **U**, dorsal and **V**, posterior views. **Abbreviations**: **aaf**, accessory articular fossa; **aap**, accessory articular process; **acdl**, anterior centrodiapophyseal lamina; **aof**, antorbital fossa; **di**, diapophysis; **fo**, foramen; **h**, horn; **itfm**, margin of the infratemporal fenestra; **mf**, medial foramen; **nc**, neural canal; **ns**, neural spine; **ob**, orbital boss; **oc**, olfactory canal; **om**, orbital margin; **pa**, parapophysis; **pcdl**, posterior centrodiapophyseal lamina; **poz**, postzygapophysis; **sr1**, first sacral rib; **st**, spine table; **stf**, supratemporal fossa; **stfm**, margin of the supratemporal fenestra. Scale bars equal 1 cm.

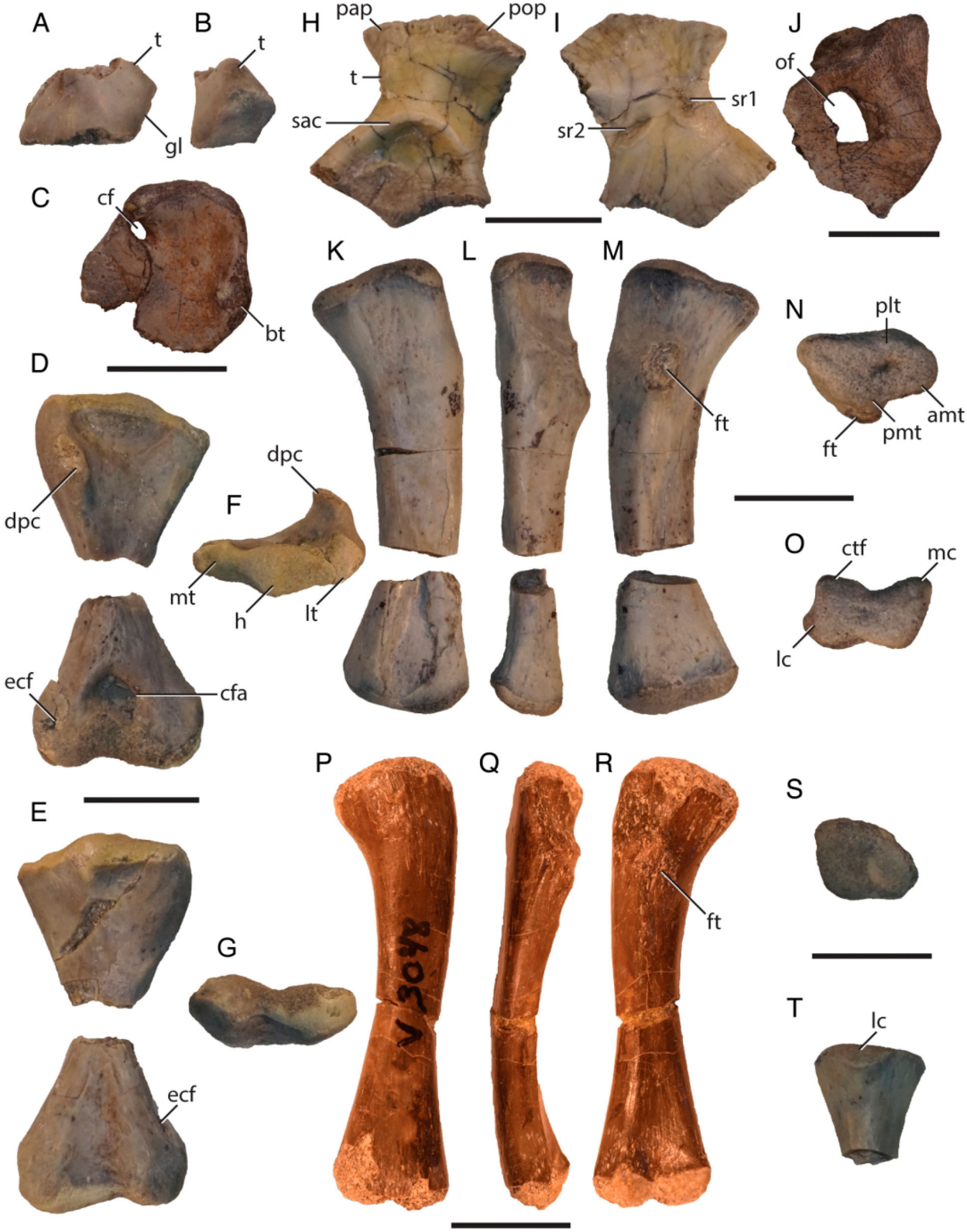

FIGURE 4. *Acaenasuchus geoffreyi*, appendicular elements. **A**, **B**, PEFO 40720, proximal end of a scapula in **A**, lateral and **B**, posterior views. **C**, UCMP 285851, partial coracoid in lateral view. **D**–**G**, PEFO 40739, right humerus in **D**, anterior, **E**, posterior, **F**, proximal, and **G**, distal views. **H**, **I**, PEFO 40731, left ilium in **H**, lateral and **I**, medial views. **J**, UCMP 285841, proximal end of a pubis in lateral view. **K**–**O**, PEFO 38763, left femur in **K**, anterior, **L**, lateral, **M**, posterior, **N**, proximal, and **O**, distal views. **P**–**R**, MNA V3048, left femur in **P**, anterior, **Q**, lateral, and **R**, posterior views. **S**, **T**, PEFO 40731, proximal end of left tibia in **S**, proximal and **T**, posterior views. **Abbreviations**: **amt**, anteromedial tuber; **bt**, biceps tuber; **cf**, coracoid foramen; **cfa**, cuboid fossa; **ctf**, crista tibiofibularis; **dpc**, deltopectoral crest; **ecf**, ectepicondylar foramen; **ft**, attachment for the M. caudofemoralis longus; **gl**, glenoid; **h**, head; **lc**, lateral condyle; **lt**, lateral tuberosity; **mc**, medial condyle; **mt**, medial tuberosity; **of**, obturator foramen; **plt**, posterolateral tuber; **pmt**, posteromedial tuber; **pap**, preacetabular process; **pop**, postacetabular process; **sac**, supraacetabular crest; **sr1**, first sacral rib; **sr2**, second sacral rib; **t**, tubercle. Scale bars equal 1 cm.

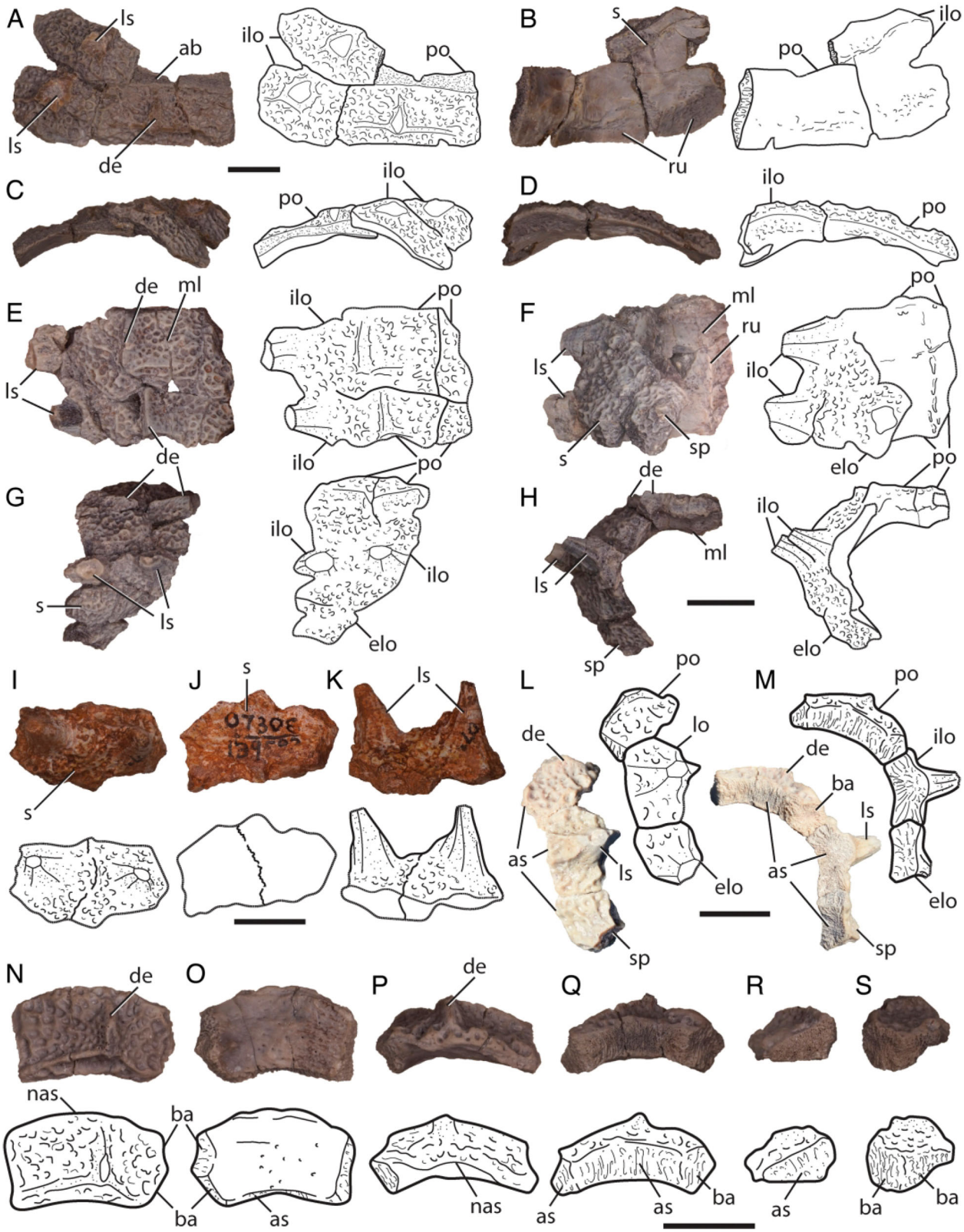

FIGURE 5. *Acaenasuchus geoffreyi*, osteoderms. **A**–**D**, PEFO 40740, left cervical osteoderm in **A**, dorsal, **B**, ventral, **C**, anterior, and **D**, posterior views. **E**–**H**, PEFO 38737, caudal osteoderm in **E**, dorsal, **F**, ventral, **G**, lateral, and **H**, posterior views. **I**–**K**, UCMP 139582, co-ossified lateral osteoderm in **I**, dorsal, **J**, ventral, and **K**, lateral views. **L**, **M**, PEFO 40702, partial sacral/anterior caudal osteoderm ring in **L**, dorsal and **M**, posterior views. **N**–**S**, PEFO 40702, complete right pelvic/anterior caudal paramedian osteoderm in **N**, dorsal, **O**, ventral, **P**, anterior, **Q**, posterior, **R**, medial, and **S**, lateral views. **Abbreviations**: **ab**, anterior bar; **as**, articulating surface; **ba**, beveled articulating surface; **de**, dorsal eminence; **elo**, external lateral osteoderm; **ilo**, internal lateral osteoderm; **ls**, lateral spike; **ml**, midline; **nas**, non-articulating surface; **po**, paramedian osteoderm; **ru**, rugosity; **s**, suture; **sp**, spike. Dashed lines indicate broken margins. Scale bars equal 1 cm.

number of specimens in UCM and UMNH collections are known from the Red Canyon area in San Juan County, southeastern Utah, within the lower Monitor Butte Member (Dubiel, 1987; Parrish and Good, 1987; Parrish, 1999). Their precise stratigraphic relationship to specimens from Arizona is unclear, but their stratigraphic position ~5 m above the Shinarump Member (Dubiel, 1987), the lithology of the Monitor Butte Member, and fossil occurrences suggest a correlation with the lower part of the Blue Mesa Member at PEFO (Martz et al., 2017). Other uncatalogued specimens from this area were noted by one of us at MCZ (R.B.I., pers. observ.), but we have not inventoried them. See Supplementary Data 1 for a list of localities. Detailed locality information and field notes are available in the museum archives at MNA, PEFO, SMU, UCM, UCMP, and UMNH to qualified researchers.

Several high-precision detrital zircon U-Pb ages from PEFO and the St. Johns region constrain the highest and lowest occurrences of *Acaenasuchus geoffreyi* in Arizona (Fig. 1). The *Placerias* Quarry (UCMP A269) in the lower part of the Sonsela Member is constrained by a maximum depositional age 219.39 ± 0.12 Ma and the bone-bearing horizon at PFV 449 (the Salado Site) directly overlies a sandstone dated to a maximum depositional age of 221.6 ± 1.4 Ma (Ramezani et al., 2011, 2014). The specimens from the upper part of the Blue Mesa Member at PEFO are constrained by maximum depositional ages of 223.036 ± 0.059 Ma (TPS sample) and 220.123 ± 0.068 Ma (SS-7 sample) (Ramezani et al., 2011; Atchley et al., 2013). However, recent U-Pb age-calibrated magnetostratigraphy from PEFO suggests that ages from the lower part of the Sonsela Member and upper part of the Blue Mesa Member may be biased by redeposited zircons that are significantly older than the depositional age (Kent et al., 2018, 2019). This magnetic polarity age model suggests that the upper Blue Mesa Member localities are ~219–217 Ma, and the lower Sonsela Member localities are ~217–216 Ma. Regardless of exact age, all known occurrences of *Acaenasuchus geoffreyi* are from the middle Norian Stage.

DESCRIPTION

Cranium and Mandible

Maxilla—A partial left maxilla is preserved in PEFO 43699 (Fig. 3I, J). It includes part of the tooth-bearing posterior process and three alveoli, two of which contain nearly complete teeth. The lateral side of the maxilla is ornamented with longitudinal grooves below the antorbital fossa and irregular ridges and pits above it (Fig. 3I). A low longitudinal ridge is present on the lateral surface, but it is not as prominent as that of *Revueltosaurus callenderi* (PEFO 34561) and some aetosaurs such as *Aetosaurus ferratus* (Schoch, 2007); *Stagonolepis robertsoni* (Walker, 1961) and *Longosuchus meadei* (TMM 31185-98) (Nesbitt, 2011). The anteromedial process of the maxilla is short and projects ventral to the alveolar margin. The ventral margin of the antorbital fenestra is concave up and forms the dorsal edge of the element.

The two fully erupted teeth are ankylosed onto the alveolar margin by 'attachment bone' (Bertin et al., 2018), but the empty alveolus exhibits obvious thecodont implantation. This is the first report of 'ankylothecodonty' (sensu Chatterjee, 1974) in pseudosuchian archosaurs, a group which has only been noted to have teeth attached into sockets via gomphosis (e.g., Leblanc et al., 2017), although the mode of tooth implantation has not been described for most Triassic pseudosuchians with tooth bearing elements. Ankylothecodonty is reported in silesaurid dinosauromorphs (Nesbitt et al., 2010; Kammerer et al., 2011; Langer and Ferigolo, 2013; Langer et al., 2013; Agnolin and Rozadilla, 2018) as well as non-archosaur archosauromorphs including rhynchosaurs (Chatterjee, 1974; Benton, 1984) and allokotosaurs (Murry, 1987; Sues, 2003; Nesbitt et al., 2015; Sengupta et al., 2017).

The teeth are labiolingually compressed and are mesiodistally widest near their apicobasal midpoint (Fig. 3J). Apically, the teeth taper to a rounded tip. The teeth are similar to the maxillary teeth of *Revueltosaurus callenderi* (PEFO 34561) in that they contain broad denticles along the mesial and distal carinae; however, the teeth of *Acaenasuchus geoffreyi* are not as labiolingually wide basally as those of *Revueltosaurus callenderi*. The anatomy of the maxillary teeth is variable in aetosaurs, from the mediolaterally compressed, curved teeth found in *Aetosauroides scagliai* (Brust et al., 2018) to the bulbous teeth of *Desmatosuchus smalli* (Small, 2002). The maxillary teeth of *Typothorax coccinarum* (PEFO 38001/YPM VP.58121) include a labiolingually compressed leaf-shaped morphology more similar to what is found in *Revueltosaurus callenderi* and *Acaenasuchus geoffreyi* except that in *T. coccinarum* defined denticles are lacking on these teeth (Reyes et al., in review).

Jugal—The lateral surface of the jugal (UCMP 285903) is heavily ornamented with anastomosing ridges and corresponding pits. It is anteroposteriorly long (Fig. 3G, H); the ventral margin of the orbit forms most of the dorsal edge of the bone, similar to that of the New Haven Formation erpetosuchid, AMNH FARB 29300 (Olsen et al., 2000:fig. 2) and different from aetosaurs where the anterior extension of the postorbital excludes much of the jugal from participation in the orbit rim (e.g., *Aetosaurus ferratus*; Schoch, 2007). The bone is dorsoventrally thin and tapers posteriorly, unlike the jugal of *Parringtonia gracilis* (NMT RB28; Nesbitt et al., 2018b:fig. 2g), *Revueltosaurus callenderi* (PEFO 34561) and aetosaurs such as *Aetosaurus ferratus* (SMNS 5770 S-16; Schoch, 2007:fig. 3e), *Paratypothorax andressorum* (SMNS 19003; Schoch and Desojo, 2016:fig. 4b), and *Desmatosuchus smalli* (TTU-P9024; Small, 2002). A sharp longitudinal ridge occurs on the lateral side of the jugal, this feature is also present in some early theropod dinosaurs and most suchians except rauisuchids, which possess a rounded ridge (Nesbitt, 2011). The longitudinal ridge on the jugal of *Acaenasuchus geoffreyi* lies above a shallow, ventral-facing groove.

Frontal—Unlike the relatively mediolaterally wide frontal of some stagonolepidid aetosaurs *Aetosaurus ferratus* (SMNS 5770 S-8; Schoch, 2007:fig. 3a) and *Paratypothorax andressorum* (SMNS 19003; Schoch and Desojo, 2016:fig. 4b), those of *Acaenasuchus geoffreyi* (UCMP 285854) and *Revueltosaurus callenderi* (PEFO 34561) are mediolaterally narrower anteriorly than posteriorly. This is more similar to some aetosaurs such as *Desmatosuchus spurensis* (UMMP 7476) and *Stagonolepis robertsoni* (Walker, 1961). The dorsal surface of the frontal of *Acaenasuchus geoffreyi* is heavily ornamented with sharp-ridged circular and oblong pits (Fig. 3A, B). This is most similar to the ornamentation on the frontal of *Revueltosaurus callenderi* (PEFO 34561), and it differs from the frontal of *Paratypothorax andressorum* (SMNS 19003; Schoch and Desojo, 2016:fig. 4b) in which the ornamentation is not as prominent and is largely located near sutures and the lateral edge of the element. One of the most striking features of this element is the large boss that forms the dorsal margin of the orbit, which projects dorsally above the skull roof in posterior view. This boss may represent a palpebral co-ossified to the frontal, as the palpebral is widely distributed across pseudosuchian archosaurs (Nesbitt et al., 2013b); the aetosaur *Aetosaurus ferratus* (SMNS 5770; Schoch, 2007:fig. 4a, b) preserves separate supraorbital and the erpetosuchid *Pagosvenator candelariensis* (MMACR PV 036-T; Lacerda et al., 2018:fig. 3) preserves separate dorsally ornamented palpebrals. The articular surfaces for the prefrontal are anteroposteriorly longer than those for the postorbital. Two foramina are present on the ventral surface of the bone beneath the orbital boss.

Parietal—The dorsal surface of the parietal (UCMP 285903; Fig. 3C, D) is ornamented with sharp ridges and small, deep

pits, similar to the frontal, unlike the broad pits and lower ridges found on the parietal of *Doswellia kaltenbachi* (USNM 214823; Dilkes and Sues, 2009:fig. 1a) and *Rugarhynchos sixmilensis* (NMMNH P-61909; Heckert et al., 2012:fig. 3k; Wynd et al., 2020), as well as *Revueltosaurus callenderi* (PEFO 34561) and some aetosaurs (e.g., *Paratypothorax andressorum*, SMSN 19003). The dorsal surface lacks the midline crest observed in *Erpetosuchus granti* (NHMUK PV R 3139; Benton and Walker, 2002:fig. 2b) and *Parringtonia gracilis* (NMT RB28; Nesbitt et al., 2018b:fig. 3d), some ornithischian dinosaurs and 'sphenosuchian' crocodylomorphs, and shuvosaurids (Benton and Walker, 2002; Nesbitt, 2011). The squamosal process is broken but the base extends posterolaterally, unlike the laterally projecting processes of aetosaurs and some crocodylomorphs (Schoch, 2007; Nesbitt, 2011; Schoch and Desojo, 2016). The supratemporal fossa broadens anteriorly, and the articular surface for the frontal comprises an interdigitating suture.

Squamosal—The squamosal of *Acaenasuchus geoffreyi* (UCMP 285837) in dorsolateral view is only slightly longer anteroposteriorly than it is wide mediolaterally, and does not taper posterodorsally as it does in erpetosuchids (Fig. 3E; Nesbitt and Butler, 2013; Nesbitt et al., 2018), *Revueltosaurus callenderi* (PEFO 34561), and the aetosaurs *Desmatosuchus smalli* (TTU-P9024; Small, 2002), *Stenomyti huangae* (DMNH 60708; Small and Martz, 2013:fig. 4), and *Aetosaurus ferratus* (SMNS 5770 S-16 and SMNS 5770 S-18; Schoch, 2007:fig. 8a). The dorsal surface is ornamented with thin ridges and small pits that together form larger ridges that radiate anteriorly and ventrally from the articulation with the parietal. The articular surfaces for the quadratojugal and the postorbital are slotted on the ventromedial surface of the bone. The articular facet for the paroccipital process of the opisthotic is broad and similar to that of *Revueltosaurus callenderi* (e.g., PEFO 34561) and aetosaurs (Nesbitt, 2011). The posterior margin of the squamosal is concave, with a small horn that projects posterodorsally.

Articular and Surangular—The surangular is co-ossified to the articular in UCMP 293853 (Fig. 3K, L). The lateral surface of the surangular is heavily ornamented; the posterior half comprises small pits and short ridges and the anterior half has long ridges and oblong anteroposteriorly oriented pits. The medial articular foramen is present in *Acaenasuchus geoffreyi*, *Revueltosaurus callenderi* (e.g., PEFO 34561), and most other pseudosuchians (Nesbitt, 2011), but it is absent in *Desmatosuchus smalli* (TTU-P9024; Small, 2002), and *Longosuchus meadei* (TMM 31185-84b; Parrish, 1994; Nesbitt, 2011). The retroarticular process of *Acaenasuchus geoffreyi* is short and curves posterodorsally but does not project above the glenoid.

Vertebral Column

Trunk Vertebrae—The only non-sacral vertebrae that can be confidently referred to *Acaenasuchus geoffreyi* belong to the dorsal series, which we call 'trunk vertebrae,' that are consistently the same size, and include fragments of centra, neural arches, zygapophyses, and transverse processes (Fig. 3M–P; PEFO 40687, PEFO 40703, PEFO 40712, PEFO 40723, PEFO 40731, PEFO 40738, UCMP 285904) or fairly complete elements (UCMP 124548, UCMP 124551, UCMP 192558). These vertebrae preserve the parapophysis and the diapophysis on the neural arch/transverse process and lack chevron facets. The centrum is amphicoelous, and both cotyles are strongly concave (most of the UCMP specimens are worn flat). Shallow longitudinal depressions occur on the lateral sides of the centrum just under the neural arch. The centrum and the neural arch are strongly integrated into one another and there is no external trace of a suture in any of the well-preserved specimens. Trunk vertebrae neurocentral sutures close relatively later in ontogeny in pseudosuchians but timing can vary (Brochu, 1996; Irmis, 2007), so either *Acaenasuchus geoffreyi* reached skeletal maturity early in ontogeny or all the known specimens represent skeletally mature individuals. The neural arch is extremely flat and table-like (Fig. 3M, S), much like that of *Euscolosuchus olseni* (USNM 448584; Sues, 1992), and is approximately as mediolaterally wide as it is anteroposteriorly long (excluding the transverse processes). Four discrete laminae extend from the base of the transverse process to the side of the neural arch: the anterior centrodiapophyseal lamina, the posterior centrodiapophyseal lamina, the prezygadiapophyseal lamina, and the postzygadiapophyseal lamina (Wilson, 1999). The anterior centrodiapophyseal and posterior centrodiapophyseal laminae are very close to one another (Fig. 3Q) and form a small, circular centrodiapophyseal fossa (Wilson et al., 2011). The two centrodiapophyseal laminae join to form a prominent ventral strut that extends laterally down the length of the transverse process.

The mediolateral length of the transverse process is much greater than the anteroposterior length of its respective centrum (Fig. 3M–P), much like the broad transverse processes of some doswelliids and erpetosuchids (Ezcurra, 2016), a condition that may have helped support the armor carapace. This may be functionally similar to the condition in the trunk of stagonolepidid aetosaurs (e.g., Parker, 2008:fig. 11; Parker, 2016b:fig. 14), where there is a large amount of variation in the relative contribution of the transverse process and rib to the support structure (e.g., Parker, 2016a:character 40). The distal end of the transverse process is ornamented with small pits and longitudinal grooves (e.g., PEFO 40687, PEFO 40703, PEFO 40712, and PEFO 40723), similar to but not to the extent observed on the ribs of *Euscolosuchus olseni* (USNM 448590; Scheyer and Sues, 2016); there are no trunk ribs preserved in PFV 211 that unambiguously belong to *Acaenasuchus geoffreyi*, but the direct articulation of the distal end of the transverse process and proximal end of the rib suggest that these two structures were of similar anteroposterior width. The transverse process terminates in the offset circular, concave articular facets of the diapophysis and the parapophysis. The presence of the diapophysis and the parapophysis completely on the transverse process of the trunk vertebrae differs significantly from the condition found in most non-crocodylomorph pseudosuchians where the parapophysis is situated on the neural arch close to the base of the process. The pairing on the transverse process is found on in *Acaenasuchus geoffreyi*, all aetosaurs (e.g., *Desmatosuchus spurensis*, UMMP 7476), and *Alligator* (e.g., Chiasson, 1962). The functional significance of this has not been determined, but its distribution is convergent among these three taxa.

In *Acaenasuchus geoffreyi* the prezygapophyseal, centrodiapophyseal, and postzygapophyseal centrodiapophyseal fossae are subtriangular and deep. The prezygapophyses (and the postzygapophyses) lie very close to one another across the midline of each vertebra, unlike those of *Euscolosuchus olseni*, in which the zygapophyses extend anteriorly/posteriorly and laterally on tapering processes (USNM 448584; Sues, 1992:fig. 2b). The neural arch contains bilateral accessory articular structures medial to the prezygapophysis and postzygapophysis (best preserved in UCMP 192558; Fig. 3S, T). They are similar to hyposphene/hypantrum articulations found in some aetosaurs (*Desmatosuchus spurensis*, MNA V9300; *Scutarx deltatylus*, PEFO 34045) and other archosaurs (see Stefanic and Nesbitt, 2019), but they do not occur on the midline. The anterior component is a dorsal subtriangular fossa found medial to the prezygapophysis and the posterior component is a ventral subtriangular process medial to the postzygapophysis. Small, circular fossae occur on the midline between both pairs of zygapophyses just below the level of the base of the neural spine. The neural spine on the trunk vertebrae projects up from the middle of the flat dorsal surface of the neural arch of *Acaenasuchus geoffreyi* (similar to that of *Doswellia kaltenbachi*; USNM 244214; Dilkes and Sues, 2009:fig. 4a; Ezcurra, 2016)

and is robust yet dorsoventrally short, much like that of *Euscolosuchus olseni* (USNM 448584; Sues, 1992:fig. 2a).

Sacral Vertebrae—Most of the morphology of the first primordial sacral vertebra can be reconstructed from portions attached to fragmentary sacral ribs (PEFO 38761, PEFO 40704, and UCMP 285840), partial sacral centra (PEFO 40723), and half of a sacral vertebra (Fig. 3U, V; UCMP 192558). These specimens are identified as the first primordial sacral by the rounded distal end of the sacral rib that does not extend posterolaterally (p. 115 of Nesbitt, 2011). The centrum is amphicoelous and dorsoventrally short. An anteroposteriorly long depression separates the centrum from the sacral rib in ventrolateral view. The anterior face of the centrum does not project anteriorly past the anteriormost extent of the sacral rib. The sacral rib is robust and is situated only on the anterior half of the centrum; it is waisted near the centrum where anterior and posterior fossae are present at its base but is anteroposteriorly expanded distally. In lateral view, most of the sacral rib is round in outline except for the posterior edge, which tapers posteriorly. The neural arch is low, and the zygapophyses are only separated from each other by a thin midline slot. The neural spine is very short dorsoventrally, and it terminates in a slightly concave 'table' that is bifurcated anteriorly and slopes ventrally posteriorly (Fig. 3U, V). Flat neural spine 'tables' are also present on the precaudal vertebrae of a number of reptile lineages, including tanystropheids, phytosaurs, ornithosuchids, *Revueltosaurus callenderi*, aetosaurs, stem-paracrocodylomorphs, and dinosaurs (Nesbitt, 2011; Pritchard et al., 2015; Marsh and Rowe, 2018; von Baczko et al., 2020), but they are mediolaterally narrower than those of *Acaenasuchus geoffreyi* (UCMP 192558) and *Euscolosuchus olseni* (USNM 448584; Sues, 1992:fig. 2a). A concave dorsal surface of the neural spine is also present in erpetosuchids (Ezcurra et al., 2017).

Pectoral Girdle and Forelimb

Scapula—Only the most proximal portion of the scapula has been found (PEFO 40720), including the glenoid region and the articulation with the coracoid (Fig. 4A, B). A small, low tubercle (origin of the M. triceps; Gower, 2003; Gower and Schoch, 2009; Nesbitt, 2011) is present just dorsal to the glenoid on the posterior surface of the scapula. This is an intermediate morphology compared to the raised, flat tubercle of *Revueltosaurus callenderi* (e.g., PEFO 34561 and PEFO 41409) and the more elongate, raised knob in *Prestosuchus chiniquensi*s (BSP XXV 1-3/5-11/28-41/49), *Batrachotomus kupferzellensis* (SNMS-BSPG 80271), and *Alligator mississippiensis* (p. 120 of Nesbitt, 2011). In aetosaurs such as *Desmatosuchus smalli* (TTU-P9023), *Typothorax coccinarum* (TTU-P9214), and *Neoaetosauroides engaeus* (PVL 3525) this tubercle is also reduced in size similar to *Acaenasuchus geoffreyi*.

Coracoid—The proximal portion of the coracoid (UCMP 285851) preserves the glenoid and the articulation with the scapula; the element is subcircular in outline (Fig. 4C). The coracoid foramen is sub-elliptical and is positioned close to the articular surface for the scapula. The 'biceps tuber' (Nesbitt, 2011) on the posteroventral portion of the coracoid below the glenoid is oblong and resembles the condition in stagonolepidid aetosaurs, such as *Desmatosuchus smalli* (TTUP 9023; Small, 1985), *Stagonolepis olenkae* (ZPAL AbIII 694; Lucas et al., 2007:fig. 5a), *Stagonolepis robertsoni* (NHMUK PV R 4784; Walker, 1961:fig. 12c), and *Typothorax coccinarum* (UCMP 34255; Martz, 2002), in contrast to the less prominent tuber of *Revueltosaurus callenderi* (e.g., PEFO 34561).

Humerus—Preserved specimens of the humerus include complete proximal and distal ends but lack the mid-diaphysis (Fig. 4D–G; PEFO 40693, PEFO 40704, and PEFO 40739). Three bulbous structures are observed on the head of the humerus in proximal view (Fig. 4F); the median humeral head is larger than the lateral and medial tuberosities. The medial tuberosity is the largest of these in *Revueltosaurus callenderi* (e.g., PEFO 34561). The medial corner of the proximal end of the humerus is gently expanded in anterior view like in some aetosaurs (e.g., *Aetosauroides scagliai*, PVL 2073; Parker, 2016a) but unlike the prominent medial deflection observed in *Stagonolepis olenkae* (ZPAL AbIII 1175; Lucas et al., 2007:fig. 5e; Parker, 2016a), *Longosuchus meadei* (TMM 31185-84b; Long and Murry, 1995), and *Revueltosaurus callenderi* (PEFO 34561). A semicircular fossa is present just beneath the articular surface of the humeral head in anterior view, similar to that present in *Revueltosaurus callenderi* (PEFO 34561). The deltopectoral crest is fairly short proximodistally and projects anterolaterally to form a rounded subtriangular outline in lateral view. The ectepicondylar flange of *Acaenasuchus geoffreyi* completely encloses the ectepicondylar foramen like it does in most aetosaurs (except *Aetosaurus ferratus*; SMNS 5770 S-5; Schoch, 2007:fig. 10f; Parker, 2016a). This feature is found on some individuals of *Revueltosaurus callenderi* (e.g., PEFO 34561) but in specimens the flange does not completely close and forms an ectepicondylar groove (e.g., PEFO 34269). A subcircular 'cuboid fossa' is present on the distal end of the humerus in anterior view (Langer et al., 2007), and the radial and ulnar condyles are subequal in size in distal view.

Pelvic Girdle and Hind Limb

Ilium—The ilium is represented by several specimens (PEFO 16630, PEFO 40720, PEFO 40731, UCMP 192559). The 'neck' between the acetabulum and the iliac blade of *Acaenasuchus geoffreyi* (Fig. 4H, I) is dorsoventrally tall relative to the anteroposterior width of the acetabulum, similar to most stagonolepidids in which there is some variation in how this feature is expressed (Parker, 2008, 2016b). In *Acaenasuchus geoffreyi* and *Typothorax coccinarum* (UCMP 122683; Small, 1985; Martz, 2002), the distance between the top of the acetabulum and the base of the preacetabular process is quite large, resulting in an almost obtuse angle between the two. In *Aetosaurus ferratus* (SMNS 5770 S-22; Schoch, 2007:fig. 11b), *Neoaetosauroides engaeus* (PVL 3525; Desojo and Báez, 2005:fig. 2c), and *Calyptosuchus wellesi* (UMMP 13950; Parker, 2018a), this distance and angle is smaller, more similar to *Revueltosaurus callenderi* (e.g., PEFO 34561) and other non-aetosaurs (e.g., the erpetosuchid *Tarjadia ruthae*; CRILAR-Pv 478; Ezcurra et al., 2017:fig. 2j). However, in all stagonolepidids and *Acaenasuchus geoffreyi*, the distance between the posteroventral corner of the ischial peduncle and the base of the postacetabular process is quite large, whereas it is smaller in *Revueltosaurus callenderi* and other pseudosuchians.

The lateral surface of the ilium lacks a crest dorsal to the supraacetabular crest that divides the preacetabular and postacetabular processes from one another in paracrocodylomorphs (Nesbitt, 2011), but does possess a small tubercle between the supraacetabular crest and the preacetabular process (Fig. 4H; preserved in PEFO 40720 and UCMP 192559), which is not present in *Revueltosaurus callenderi* (e.g., PEFO 34561, PEFO 35316) or aetosaurs (Nesbitt, 2011) except *Aetosaurus ferratus*, in which larger specimens may preserve a similar feature (SMNS 5770 S-22; Schoch, 2007:fig. 11b). The preacetabular process is very short and pointed anteriorly similar to the plesiomorphic condition in *Revueltosaurus* (Parker et al. 2005:fig. 3c), *Tarjadia ruthae* (CRILAR-Pv 478; Ezcurra et al. 2017:fig. 2j), and most early archosaurs (e.g., p. 133 of Nesbitt, 2011), in contrast with the more elongate preacetabular processes of stagonolepidids, poposauroids, and early crocodylomorphs (e.g., Nesbitt, 2011:figs. 33, 34). The broken base of the postacetabular process extends posterolaterally, unlike in *Revueltosaurus callenderi* and the erpetosuchid *Tarjadia ruthae* (CRILAR-Pv

478; Ezcurra et al., 2017:fig. 2j), in which the postacetabular process projects posteriorly. Despite its being broken in PEFO 40731, it is evident that the blade and postacetabular process of the ilium does not extend as dramatically posterolaterally as that of *Doswellia kaltenbachi* (USNM 244214; Dilkes and Sues, 2009:fig. 14a). Two prominent rib attachment scars are present on the medial surface of the ilium (Fig. 4I). Both are situated longitudinally near the narrowest portion of the ilium between the acetabular region and the dorsal blade. The anterior scar is subcircular and the posterior scar is larger and subtriangular. Their shape and position indicate they are the articular surfaces for the ribs of the two primordial sacral vertebrae (pp. 115–118 of Nesbitt, 2011). Based on these muscle scars and the shape and orientation of the sacral ribs, the ilium of *Acaenasuchus geoffreyi* was oriented vertically like that of most archosauromorphs, not ventrolaterally deflected like the condition in some aetosaurs (e.g., *Aetosaurus scagliai* [PVL 2073], *Scutarx deltatylus*, PEFO 34919, and *Typothorax coccinarum*, PEFO 33967; Parker, 2016b) and non-poposauroid paracrocodylomorphs (Nesbitt, 2011). *Revueltosaurus callenderi* (PEFO 34561), and some other aetosaurs including *Stagonolepis robertsoni* (Walker, 1961) and *Desmatosuchus spurensis* (MNA V9300; Parker, 2008), have a more vertically oriented ilium as in *Acaenasuchus geoffreyi*.

Pubis—Only the proximal portion of the pubis is preserved in known specimens (PEFO 40693, UCMP 285841). The iliac and ischiadic pedicles are continuous with one another (Fig. 4J) and are not separated by a gap as they are in dinosauriforms and paracrocodylomorphs (Nesbitt, 2011). Only the obturator foramen perforates the pubis (Fig. 4J), unlike in *Stagonolepis robertsoni* (NHMUK PV R 4793; Walker, 1961; Parker, 2018b) and *Scutarx deltatylus* (PEFO 31217; Parker, 2016a, 2016b) in which there is an accessory foramen. The obturator foramen of *Acaenasuchus geoffreyi* appears to vary in size (larger in UCMP 285841, smaller in PEFO 40693).

Femur—One complete left femur with worn articular ends (MNA V3048; Fig. 4P–R), most of another left femur missing just a small portion of the midshaft (PEFO 38763; Fig. 4K–O), and several proximal and distal ends of femora (PEFO 40734, PEFO 40720, PEFO 40696) are preserved. The femur is fairly robust and relatively short. It is weakly sinusoidal in anterior view and is concave posteriorly in lateral view. The femoral head is blocky and in proximal view preserves small anteromedial and posterolateral tubera and a larger posteromedial tuber similar to other non-paracrocodylomorph suchians (Fig. 4N; Nesbitt, 2011). A short groove is present on the proximal surface in the best-preserved specimen (PEFO 38763). Such a groove is at least partly an ontogenetically variable character (p. 613 of Griffin, 2018) and it is variably present in non-ornithodiran avemetatarsalians (Nesbitt et al., 2017), dinosauriforms (Nesbitt, 2011; Griffin, 2018), *Ornithosuchus longidens* (NHMUK PV R 3561; Walker, 1964:fig. 12d), and paracrocodylomorphs (Nesbitt, 2011:150), but not *Revueltosaurus callenderi* (e.g., PEFO 34561) or the aetosaurs *Typothorax coccinarum* (UCMP 34238; Nesbitt, 2011:fig. 38; Nesbitt, 2011), *Stagonolepis robertsoni* (NHMUK PV R 581; Walker, 1961), and *Longosuchus meadei* (TMM 31185-84a; Sawin, 1947). The attachment for the *M. caudofemoralis longus* ('fourth' trochanter) is situated proximally on the posterior surface of the femoral shaft just below the femoral head (Fig. 4M, R), and is a rounded, rugose knob, unlike the straighter mound of *Revueltosaurus callenderi* (e.g., PEFO 34561 and PEFO 34269). At midshaft, the cortical wall is relatively thin compared to the diameter of the element (the ratio is between 0.27 and 0.28 in PEFO 38763). This is more similar to dinosauromorphs and poposauroids than other archosaurs (Nesbitt, 2011), but may relate to the diminutive size of *Acaenasuchus geoffreyi*, given that this character state often scales positively with body size in amniotes (e.g., Wall, 1983; Currey and Alexander, 1985; Ray and Chinsamy, 2004; Botha-Brink and Angielczyk, 2010; Mukherjee, 2015). The angle between the crista tibiofibularis and the lateral condyle in distal view is obtuse (Fig. 4O), and the medial condyle tapers to a point like it does in non-ornithodiran avemetatarsalians, *Revueltosaurus callenderi*, stagonolepidid aetosaurs, and some non-loricatan paracrocodylomorphs (excluding shuvosaurids; Nesbitt, 2011; Nesbitt et al., 2017). The medial and lateral condyles are weakly divided by the wide shallow fossae in posterior and distal views (Fig. 4M, O), and the anterior surface of the distal end of the femur is smooth.

Tibia—The proximal end of the tibia is subelliptical in proximal view (PEFO 40731; Fig. 4S, T) and preserves the medial and lateral condyles that are aligned parallel to each other along the posterior margin of the element; the lateral condyle is depressed laterodistally as in other pseudosuchians (Nesbitt, 2011), including *Revueltosaurus callenderi* (PEFO 34273) and aetosaurs (e.g., *Calyptosuchus wellesi*, UCMP 25887). The tibia lacks a prominent cnemial crest, similar to *Revueltosaurus callenderi* and aetosaurs (Nesbitt, 2011; Parker, 2018a).

Osteoderms

The hypodigm material described by Long and Murry (1995) represents the 'typical' aetosaur-like arrangement of paramedian and lateral osteoderms and all specimens exhibit the characteristic dorsal sculpturing and ornamentation of anastomosing ridges and pits. Overall, the paramedian osteoderms are rectangular and mediolaterally wider than anteroposteriorly long in dorsal view (e.g., the holotype specimen UCMP 139576; Fig. 2A, B; Long and Murry, 1995:figs. 117a, b, 118k, l) and the lateral osteoderms are subrounded or subhexagonal (e.g., Fig. 2J–M; Long and Murry, 1995:figs. 117d, 118a). Long and Murry (1995) inferred how osteoderm shape varied relative to body position in their diagnosis of *Acaenasuchus*, but did not actually assign specific specimens to specific anatomical regions in the subsequent description.

During our examination of the original hypodigm and comparison of these specimens with the new PEFO fossils, we noted extensive variation in shape, size, and articulation patterns for the osteoderms of *Acaenasuchus geoffreyi*. Based on anteroposterior carapacial variation trends observed in stagonolepidid aetosaurs (e.g., Parker, 2005b, 2007), this allows us to classify *Acaenasuchus* osteoderms by region. Ideally, carapacial regions should be determined by which vertebrae are roofed by specific osteoderms (e.g., Long and Ballew, 1985; Desojo et al., 2013), but in the absence of vertebra-osteoderm association in *Acaenasuchus geoffreyi*, we designate regions using comparisons with similar regionalized osteoderms in aetosaurs and *Revueltosaurus callenderi*. Further support for hypothesized carapacial regions comes from new PEFO specimens that are either articulated or co-ossified to one another. The cervical region is characterized by shorter paramedian osteoderms that interlock with a pair of co-ossified lateral osteoderms (Fig. 6A, B), the trunk region includes the 'typical' paramedian + lateral osteoderm pair with the widest paramedian osteoderms in the carapace (not co-ossified; Fig. 6A, B, D), and the pelvic/anterior caudal region includes rings of interlocking serial rows (Fig. 6A, B, E).

Some features are shared across osteoderms despite the serial position within the carapace. The dorsal ornamentation of the paramedian and lateral osteoderms is similar (and similar to the ornamented skull bones described above), consisting of subcircular to oblong pits radiating away from the dorsal eminence or lateral spike, with relatively more subcircular pits closer to the dorsal eminence or lateral spike (Fig. 2A, J, F). Each subcircular pit contains a foramen. The dorsal eminence and lateral spike are covered in foramina. This pattern is very similar to that of *Doswellia kaltenbachi* (USNM 244214; Dilkes and Sues, 2009: fig. 10) and *Euscolosuchus olseni* (e.g., USNM 448587), but different from *Revueltosaurus callenderi* (e.g., PEFO 34561) in which

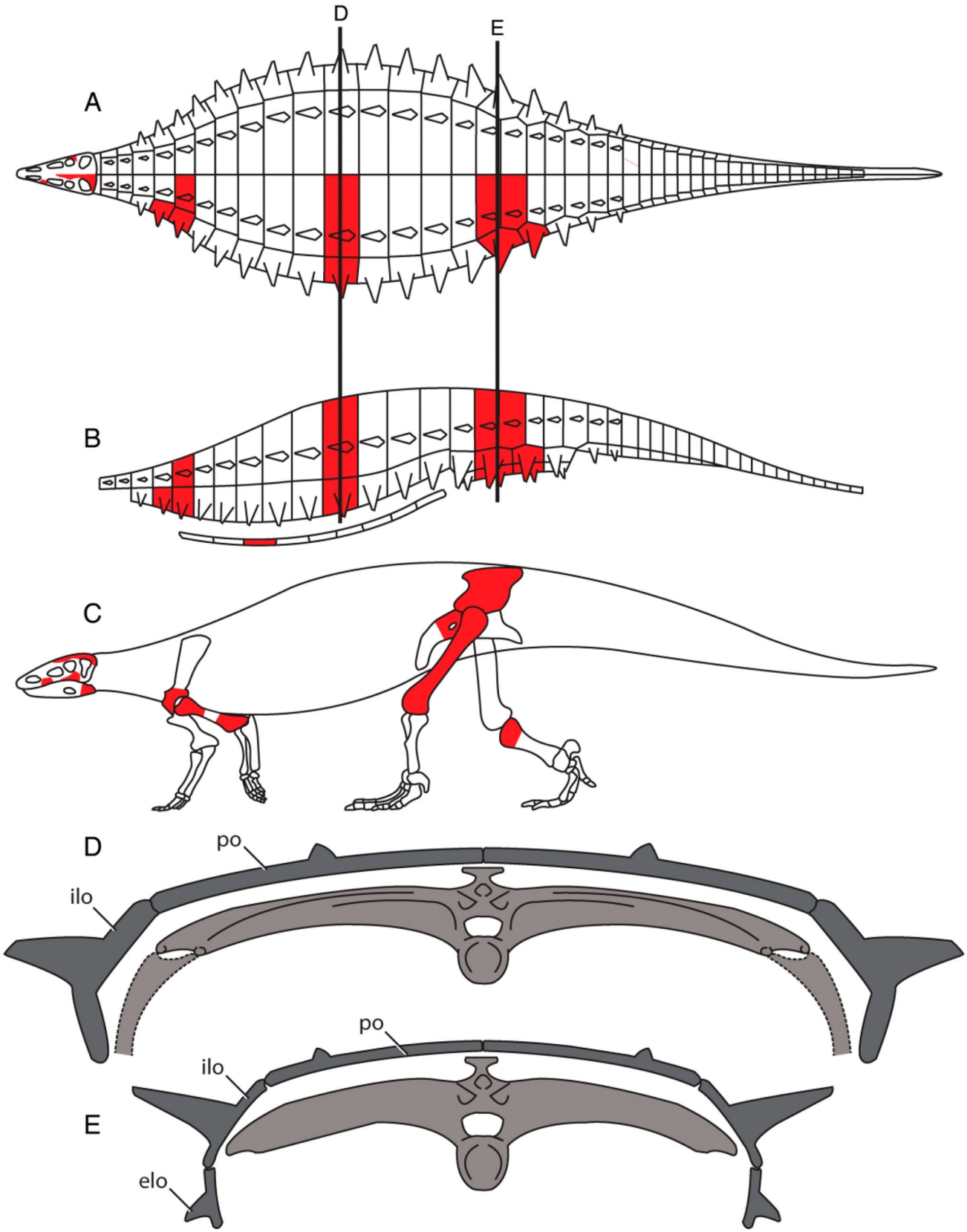

FIGURE 6. *Acaenasuchus geoffreyi*, reconstruction of the skeleton and the carapace. **A**, **B**, carapace in **A**, dorsal and **B**, left lateral views, **C**, skeleton in left lateral view. **D**, **E**, coronal sections of carapace through **D**, trunk, and **E**, sacral regions. Shaded regions in **A**–**C** represent known skeletal elements among UCMP, PEFO, and MNA specimens. Skeletal reconstruction modified from Heckert et al. (2010). Not to scale. **Abbreviations**: **elo**, external lateral osteoderm; **ilo**, internal lateral osteoderm; **po**, paramedian osteoderm.

the depressions are more circular and evenly spaced (e.g., PEFO 34561) and aetosaurs, which generally have either more widely spaced circular pits (*Typothorax coccinarum*) or a pattern of elongate grooves and pits (e.g., *Desmatosuchus spurensis*, *Calyptosuchus wellesi*) (Long and Ballew, 1985; Parker, 2008). The ventral surface of the osteoderms of *Acaenasuchus geoffreyi* is mostly smooth except for the occasional foramen or rugose patch on the posterior margin that articulates with the dorsal surface of the anterior bar of the subsequent osteoderm (Fig. 2G, K). These rugose patches are also observed on the osteoderms of *Euscolosuchus olseni* (e.g., USNM 448587). The lateral margins of the paramedian osteoderms are sigmoidal. Medially, a paramedian osteoderm articulates with the adjacent paramedian osteoderm, and laterally articulates with at least one lateral osteoderm (see below); both articulation surfaces form a tongue-in-groove system (Fig. 2C, D, J, H, I). The medial edge of a paramedian osteoderm is flat where it articulates with another paramedian osteoderm, but the lateral surface is concave to articulate with the convex medial surface of the lateral osteoderm. Each paramedian osteoderm has a dorsal eminence that projects posterodorsally into a spike or "thorn" (Long and Murry, 1995:114); some dorsal eminences curve posteriorly in medial/lateral view (Fig. 2H), whereas others remain relatively straight and dorsally erect (PEFO 40742). A dorsal ridge is present on the eminence that extends from the point of the spike to the posterior margin of the anterior bar. Unlike stagonolepidid aetosaurs, in which the dorsal eminence is often positioned either near the mediolateral mid-point or closer to the medial margin of the osteoderm (Parker, 2007), in *Acaenasuchus geoffreyi* it is positioned either near the mid-point (e.g., UCMP 139576) or closer to the lateral edge of the paramedian osteoderm (e.g., PEFO 40000). This observation is confirmed by specimens of paramedian osteoderms articulated with lateral osteoderms (PEFO 40740; Fig. 6A). This is similar to the dorsal eminence of *Revueltosaurus callenderi* (e.g., PEFO 34561) and *Euscolosuchus olseni* (USNM 448587 and USNM 448582), in contrast to the condition in paramedian osteoderms of stagonolepidids. A transverse ridge extends medially and laterally away from the posterior margin of the dorsal eminence and terminates before reaching either margin of the element (Fig. 2A). An elongate posterior fossa is formed behind this ridge and under the dorsal eminence. Each paramedian osteoderm has a raised anterior bar like that of *Revueltosaurus callenderi* and most stagonolepidid aetosaurs (Parker, 2007, 2016a), in contrast to the depressed 'anterior lamina' of *Desmatosuchus spurensis* (MNA V9300; Parker, 2008), as well as the non-raised anterior bar of *Euscolosuchus olseni* (e.g., USNM 448587, USNM 448587, and USNM 448582). As mentioned above, the anterior bar of the holotype UCMP 139576 was abraded or prepared away (inset, Fig. 2A), appearing to represent a depressed lamina, which had been used to argue that *Acaenasuchus geoffreyi* was a juvenile *Desmatosuchus spurensis* (Heckert and Lucas, 2002a), but does not reflect the true condition observed throughout the carapace. The lateral osteoderms also possess a raised anterior bar (Fig. 2J, M) and a large lateral spike projecting dorsolaterally from the middle or lateral half of the osteoderm (Fig. 2J, L).

The lateral spike is triangular in dorsal view (Fig. 2J), hexagonal in cross section (Fig. 2M, F), and has a longitudinal groove posteriorly that is similar to the fossa behind the dorsal eminence and transverse ridge of the paramedian osteoderms (Fig. 2L). The overall similarity of the lateral osteoderms to those of stagonolepidids is the major reason why *Acaenasuchus geoffreyi* was originally assigned to the Aetosauria, because prior to this study lateral osteoderms of that type in pseudosuchians were only known from aetosaurs (e.g., Long and Ballew, 1985). Our new material demonstrates that although the lateral osteoderms from some regions do appear very similar to those of stagonolepidid aetosaurs in style of articulation and 1:1 correspondence with the paramedian osteoderms, in other areas of the carapace they have different articulations, including in the cervical and caudal regions forming 'armor bands.'

Cervical Region—Both paramedian and lateral osteoderms are present in the cervical region, and when they are articulated, the width of the rows tapers anteriorly (Figs. 5A, 6A). In articulated osteoderms from the cervical region (Fig. 5A–D) the lateral osteoderms are co-ossified to one another (Fig. 5B). These lateral elements articulate closely with the respective paramedian osteoderms along an interdigitating mediolateral articular surface, as well as interdigitating articular surfaces on the anterior bar of the paramedian osteoderm and ventral surface of the lateral osteoderms (Fig. 5A). In dorsal view, the lateral margin of the cervical paramedian osteoderms is angled anteromedially and forms a subtrapezoidal outline (unlike the subrectangular outline of trunk paramedians), causing the anterior taper of the lateral margin of the osteoderm rows in the cervical region (Fig. 5A). This is more similar to what is present in *Revueltosaurus callenderi* (PEFO 34561), and very different to what is present in aetosaurs. Non-desmatosuchine aetosaurs have cervical osteoderms that are mediolaterally wider than anteroposteriorly long with a posteriorly tapering lateral edge. This is because there is an anterolateral extension of the anterior bar that overlies the dorsomedial corner of the corresponding lateral osteoderms (Parker, 2007). The trapezoidal shape in *Acaenasuchus geoffreyi* more closely resembles that of desmatosuchine aetosaurs such as *Desmatosuchus* (Parker, 2005b, 2008) and *Sierritasuchus macalpini* (Parker et al., 2008) in which the osteoderms taper anteriorly; however, they are different in that these osteoderms in aetosaurs are anteroposteriorly longer than they are mediolaterally wide.

The cervical lateral osteoderms of *Acaenasuchus geoffreyi* are slightly convex and do not form strong angles like those in the trunk region. Instead, the paramedian/lateral osteoderm pair is gently dorsally arced over the neck (Fig. 5C, D). The ventrolateral margin of the cervical lateral osteoderms is tapered and does not articulate with another osteoderm. The dorsal surfaces of the anterior bars are lightly ornamented with low bumps and small, shallow pits, differing from the smooth bars found in *Revueltosaurus callenderi* and stagonolepidid aetosaurs.

Trunk Region—The paramedian osteoderms in the trunk vary in mediolateral width and include the widest paramedians of the carapace (Figs. 2A, E, F, 6A, B). For example, UCMP 139574 is 1.75 times mediolaterally wider than it is anteroposteriorly long, and for PEFO 40694 the ratio is 2.3. The ornamentation on the dorsal surface of the anterior bar is not as prominent as that of the cervical paramedians and the rows of osteoderms in the trunk are not co-ossified. The anterior margin of the trunk paramedian osteoderms is straight in some specimens (e.g., UCMP 139576) and scalloped in others (e.g., PEFO 40000; Parker, 2018a). Two small projections extend anteriorly from the anterior bar medial to the midpoint; one projection is halfway between midpoint of the osteoderm and the medial margin (similar to aetosaurs, Parker, 2016a), and the other projection occurs on the anteromedial corner of the element (Fig. 2A, F). The former projection is located more laterally in *Revueltosaurus callenderi* (e.g., PEFO 34561). The trunk paramedian osteoderms of *Acaenasuchus geoffreyi* lack the anterolateral projection observed in non-desmatosuchine stagonolepidid aetosaurs, which articulates with the lateral osteoderm (Parker, 2016a). The anterolateral corner of *Acaenasuchus geoffreyi* paramedian osteoderms is square, owing to the interdigitating suture with the lateral osteoderm. In contrast, the anterolateral corner of the holotype paramedian osteoderm of *Euscolosuchus olseni* is a long, tapered spine that projects anteriorly (USNM 448587). Both taxa differ from the condition in desmatosuchine aetosaurs where the anterolateral corner of the paramedian osteoderm is

slightly excavated to receive a small process from the corresponding lateral osteoderm (Parker, 2007, 2016a).

The lateral osteoderms in the trunk region of *Acaenasuchus geoffreyi* are not co-ossified medially with a paramedian osteoderm but articulate tightly with it across an interdigitating suture (Fig. 2J), and do not deviate from the general description above. In posterior view, the lateral osteoderm curves ventrally to form a right angle (Fig. 2L). The angle that the lateral spike projects from the lateral osteoderm varies serially along the trunk among well-preserved specimens, but without more articulated specimens with unambiguous positional data, we cannot describe how the angle changes anteroposteriorly. The ventral margin of the lateral osteoderm tapers to a non-articulating edge. Based on the condition observed in *Acaenasuchus*, we interpret *Euscolosuchus* specimen USNM 448587 as co-ossified trunk paramedian and lateral osteoderms, in which the lateral spine of *Euscolosuchus olseni* is equivalent to the lateral spike on lateral osteoderms of *A. geoffreyi*, the dorsal eminences are homologous, and the 'dorsal keel' of *Euscolosuchus olseni* is autapomorphic for that taxon (Sues, 1992). This hypothesis needs further testing via a transverse histological section or computed tomography.

Sacral/Caudal Region—Each half of a row of sacral/anterior caudal osteoderms includes a paramedian osteoderm, an internal lateral osteoderm, and an external lateral osteoderm that articulates with the ventrolateral margin of the internal lateral osteoderm (Fig. 5E–H, L, M). In fact, two rows of osteoderms articulate with one another to form rings similar to those found in Pleistocene glyptodonts (Lydekker, 1894; Carlini et al., 2008: fig. 3f; Zurita et al., 2013:fig. 2j; Arbour and Zanno, 2018:fig. 1) and the anterior caudal region of some stem turtles (Gaffney, 1985:figs. 19, 21; Gaffney, 1990:figs. 85–88, 131–132; Sterli and de la Fuente, 2011:fig. 13). When articulated, these rings taper posteriorly over the sacrum/anterior caudal region (Fig. 5A). Each ring includes two paramedian osteoderms that articulate with one another anteroposteriorly in an interdigitating articular surface (Fig. 5M, Q), unlike the cervical and trunk regions in which the anterior bar articulates with the ventral surface of the preceding osteoderm. In each sacral/anterior caudal ring, the anterior margin of the anterior paramedian osteoderm and the posterior margin of the posterior paramedian are non-articulating surfaces (Fig. 5P). The lateral side of the paramedian osteoderm is beveled to articulate with two lateral osteoderms (Fig. 5N, O, S), unlike the paramedians in the cervical and trunk regions that only articulate laterally with a single lateral osteoderm. In posterior view (Fig. 5H, M), the sacral/anterior caudal paramedian osteoderms are curved ventrolaterally over the body more so than those in the cervical and trunk regions. The lateral osteoderms in the sacral/anterior caudal region have tall, hexagonal lateral spikes that curve slightly anteriorly (Figs. 5F, K, 6A, B), similar to the spines on the sacral/caudal paramedian osteoderms of *Rioarribasuchus chamaensis* (Parker, 2007). Only partial external lateral osteoderms exist, but they are smaller than the internal lateral osteoderms, have the characteristic ornamentation found on the other osteoderms of *Acaenasuchus geoffreyi*, and have a small spike extending from near the lateral edge of the osteoderm (Fig. 5F, L). One specimen, UCMP 139582 (Fig. 6I–K), is a pair of fused anterior and posterior internal lateral osteoderms. The entire complex of paramedian, internal lateral, and external lateral osteoderms in the sacral/anterior caudal region is more robust than the osteoderms in the cervical and trunk regions, in which the osteoderms are dorsoventrally thinner. In some specimens (e.g., PEFO 40702) these rings are tightly articulated, and in others (e.g., PEFO 38737 UCMP 139582, and UCMP 175112) each osteoderm in the two-row ring is co-ossified to neighboring osteoderms.

Ventral Osteoderms—The ventral osteoderms are subsquare in dorsal outline (Fig. 2N) and their ventral surface is either flat (e.g., UCMP 175074) or possesses a central keel (e.g., UCMP 175139) (Fig. 2N, O). The keel is formed by a mediolaterally narrow ridge that is taller in one direction (presumably posteriorly) and extends to the edge of the osteoderm (Fig. 2O). No ventral osteoderms of *Acaenasuchus geoffreyi* have been found in articulation, so it is impossible to determine the number of columns. However, the ventral osteoderms of *Acaenasuchus geoffreyi* lack the anterior bars of overlapping ventral osteoderms observed in *Revueltosaurus callenderi* (e.g., PEFO 34269 and PEFO 42442/UWBM 116869) and most aetosaurs that preserve those elements (Heckert et al., 2010; Desojo et al., 2013). It is likely that the ventral osteoderms only abutted one another like those of crocodyliforms (Colbert and Mook, 1951:fig. 4, pl. 11; Brochu, 1997: fig. 15; pp 183–184 in Nesbitt, 2011) or were less directly associated with one another like those of *Stenomyti huangae* (DMNH 60708; Small and Martz, 2013:fig. 2b). It is not clear if *Acaenasuchus geoffreyi* has ventral osteoderms under the tail, as in *Stagonolepis robertsoni* (ELGNM 2018.6.2; Keeble and Benton, 2020:fig. 3a).

Additional Records

Our redescription of *Acaenasuchus geoffreyi* focuses on material from the type locality and referred specimens from nearby sites in northeastern Arizona, U.S.A. (Fig. 1). From collections made in the 1980s in the lower Monitor Butte Member (Chinle Formation) near the Blue Lizard Mine (UCM loc. 88067) in Red Canyon, southeastern Utah, U.S.A. (Parrish and Good, 1987; Dubiel, 1987). Parrish (1999:fig. 4) figured and briefly described four small osteoderms (UCM 76194) that he assigned to an indeterminate archosauriform, but compared closely with the early archosauriform *Doswellia*. These specimens possess the distinctive ornamentation of *Acaenasuchus geoffreyi*, with at least one of them preserving a dorsal eminence that does not reach the posterior margin, and a smooth anterior bar (Parrish, 1999:fig. 4). Additional material was collected from nearby sites at the same stratigraphic level by Harvard University in 1986, 1997, and 2003; these uncatalogued specimens were observed by one of us (R.B.I.) in 2007 to include additional *Acaenasuchus* osteoderm material.

More recently (2009–2018), the Utah Geological Survey revisited the MCZ site and associated outcrops, surface-collecting small vertebrate material that includes *Acaenasuchus geoffreyi* paramedian osteoderms (UMNH VP 30185, 30186, 30208, 30209, 30210, 30217) (Fig. 7A–C) and one lateral osteoderm (UMNH VP 30184) (Fig. 7D–F). These specimens are indistinguishable from equivalent elements in the type and referred material from Arizona. Particularly notable is a single proximal caudal vertebra (UMNH VP 30183) found in direct association with this material (Fig. 7G–K). The caudal vertebral column is not represented among the type locality and PEFO material, so we cannot be certain that this vertebra is assignable to *Acaenasuchus*, but its morphology is consistent with such a referral. Beyond its small size, the vertebra shares with other *Acaenasuchus* vertebrae (Fig. 3M–V) deeply amphicoelous centrum faces (Fig. 7I, J), laterally expanded transverse processes (Fig. 7G, H), and dorsally thickened proximal portions of the transverse processes where they meet the centrum (Fig. 7I, J).

The taphonomy of the Red Canyon sites is particularly intriguing, because there are several similarities with the *Acaenasuchus* type locality in the Blue Hills of Arizona. Both are dominated by small tetrapod remains, with individual skeletal elements that are typically <2–3 cm in maximum length. In addition to *Acaenasuchus*, the Blue Hills site (UCMP V7308) preserves small temnospondyl amphibian material (Long and Murry, 1995; Parker, 2005a), and teeth, osteoderms, and other bones of the small pseudosuchian *Revueltosaurus hunti* (Heckert, 2002; Heckert and Lucas, 2002b; Irmis, 2005:72; Parker, 2005a; Parker et al., 2005; Irmis et al., 2007a). The Red Canyon assemblage

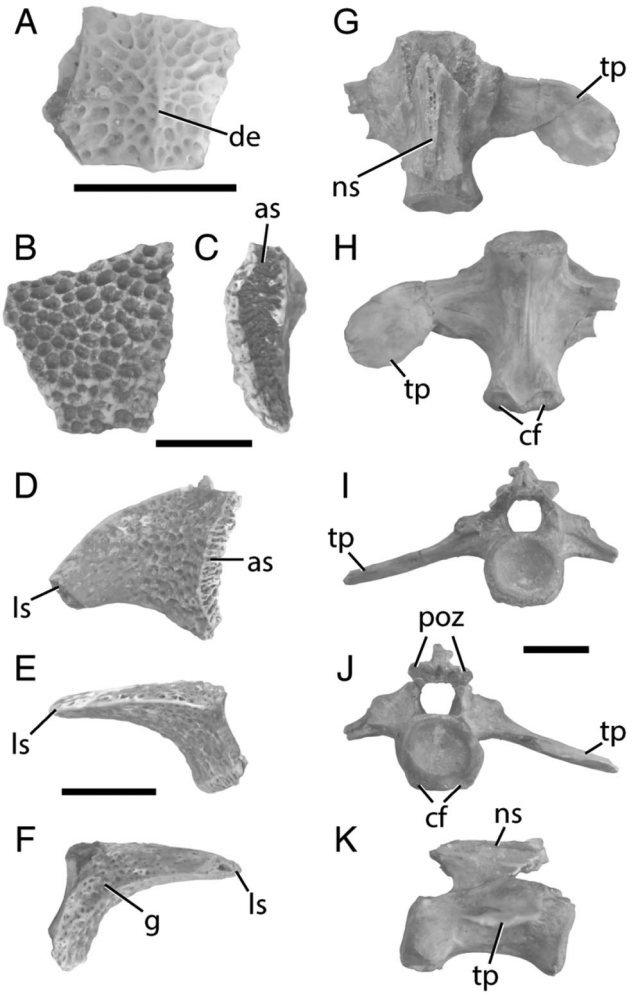

FIGURE 7. *Acaenasuchus geoffreyi*, representative specimens from the Red Canyon area of southeastern Utah, U.S.A. **A**, UMNH VP 30185, partial paramedian osteoderm in dorsal view. **B**, **C**, UMNH VP 30186, partial paramedian osteoderm in **B**, dorsal and **C**, lateral views. **D**–**F**, UMNH VP 30184, partial lateral osteoderm in **D**, ventral, **E**, anterior, and **F**, posterior views. **G**–**K**, UMNH VP 30183, caudal vertebra in **G**, dorsal, **H**, ventral, **I**, anterior, **J**, posterior, and **K**, right lateral views. **Abbreviations**: **as**, articulating surface; **cf**, chevron facets; **de**, dorsal eminence; **g**, groove; **ls**, lateral spike; **ns**, neural spine; **poz**, postzygapophysis; **tp**, transverse process. Scale bars equal 5 mm.

also contains small temnospondyls (Parrish and Good, 1987: fig. 2a; UMNH VP 30187, centra; UMNH VP 30188, jaw fragment; UMNH VP 30189, clavicle/interclavicle fragments; UMNH VP 30191, jaw fragment; UMNH VP 30214, jaw fragment), *Revueltosaurus hunti* teeth (UMNH VP 30211), osteoderms (Parrish, 1999:fig. 1, UCM 76195; UMNH VP 30190, UMNH VP 30212, UMNH VP 30213), and other elements (Parrish, 1999:figs. 2, 3, UCM 76191–UCM 76193, UCM 76195). The sedimentology of the two sites does differ; in the Blue Hills, the fossiliferous horizon is a light greenish grey matrix-supported intraformational conglomerate with granule- to pebble-sized clasts of mud rip-ups, carbonate nodules, and silty mudstone matrix (R.B.I., pers. observ., 2011), whereas the Red Canyon specimens are preserved in tan carbonate lenses at the base of a tan to brown mottled mudstone (Dubiel, 1987; Parrish and Good, 1987). Nevertheless, the commonalities in body size and taxonomic content may suggest a similar habitat or community.

Osteohistology

Our main goal in examining the bone histology of *Acaenasuchus* is to assess its skeletal maturity, given that some previous authors have explicitly hypothesized that this material represented juvenile specimens of the stagonlepidid aetosaur *Desmatosuchus* (Heckert and Lucas, 2002a). We selected osteoderms (Fig. 8) for our analysis because: (1) they are the most plentiful element in the known hypodigm; and (2) previous studies demonstrate that osteoderms from both extant and extinct pseudosuchian archosaurs record valuable skeletochronological data (e.g., Hutton, 1986; Games, 1990; Woodward and Moore, 1992; Tucker, 1997; Erickson and Brochu, 1999; Parker et al., 2008; Cerda and Desojo, 2011; Cerda et al., 2013, 2018; Taborda et al., 2013; Scheyer et al., 2014). This previous work also showed that longitudinal sections through the dorsal eminence (or equivalent) provide one of the most complete records of growth (Hutton, 1986; Tucker 1997; Cerda and Desojo, 2011; Taborda et al., 2013; Cerda et al., 2018), so we followed this strategy in our work (Fig. 8A–D) in sampling one paramedian osteoderm (UCMP 175103) and one lateral osteoderm (UCMP 175114).

Both osteoderms are dominated by compact cortical bone, with a small number of large vascular endosteal spaces (Fig. 8B, D, F), in contrast with the large number of small vascular spaces in stagonolepidid aetosaurs (Parker et al., 2008; Cerda and Desojo, 2011; Scheyer et al., 2014; Cerda et al., 2018). This cortical bone comprises parallel-fibered tissue organized into thin laminae or layers (Fig. 8B, D, F), but does not possess the 'crossed' parallel-fibered variant observed in other aetosaurs (Cerda et al., 2018). Overall, the cortex is largely avascular, with only a few large simple canals and primary osteons oriented perpendicular to the plane of section (mediolaterally within the osteoderm). The ornamented surface of the osteoderms is underlain by undulating sets of dense laminae; though this is similar to the condition in other aetosaurs, *Acaenasuchus* lacks any evidence of the 'cut and fill' structure caused by resorption and deposition between sets of laminae that is observed in stagonolepidid aetosaurs (e.g., Cerda and Desojo, 2011:figs. 3a, b, 4c; Scheyer et al., 2014: figs. 6d, 7, 9, 10; Cerda et al., 2018) and crocodyliforms (e.g., de Buffrénil, 1982; Hua and de Buffrénil, 1996). As with other pseudosuchians (Hutton, 1986; Games, 1990; Parker et al., 2008; Cerda and Desojo, 2011; Scheyer et al., 2014; Cerda et al., 2018), growth marks are particularly apparent in the cortex of the ventral portion of the osteoderm (Fig. 8B, D). These are most apparent in the longitudinal section of UCMP 175114, which displays a minimum of seven growth marks (Fig. 8D); if interpreted as lines of arrested growth (LAGs), they would indicate a minimum age of seven years. In UCMP 175103, growth marks are also present, but it is more difficult to distinguish them from prominent laminae (Fig. 8B).

Overall, the combination of parallel-fibered bone with laminae and sparse simple vascular canals is an indicator of relatively slow skeletal growth (e.g., Francillon-Vieillot et al., 1990; de Margerie et al., 2002, 2004; Cubo et al., 2008). This is not entirely unexpected, as growth rate scales positively with body size (e.g., Case, 1978), and so one would expect a small-bodied animal (i.e., *Acaenasuchus*) to grow slower than a larger one (e.g., many stagonolepidid aetosaurs). The relatively avascular compact structure with a small number of large endosteal spaces may also be a function of body size, as this condition is also present in the small-bodied pseudosuchian *Revueltosaurus callenderi* (Scheyer et al., 2014), though Cerda et al. (2018) hypothesized it reflected the plesiomorphic character state for Aetosauria and its sister groups. Therefore, histological indicators of slow growth cannot be used alone to infer skeletal maturity stage. That said, several observed osteohistological characters do provide evidence for the ontogenetic stage of these

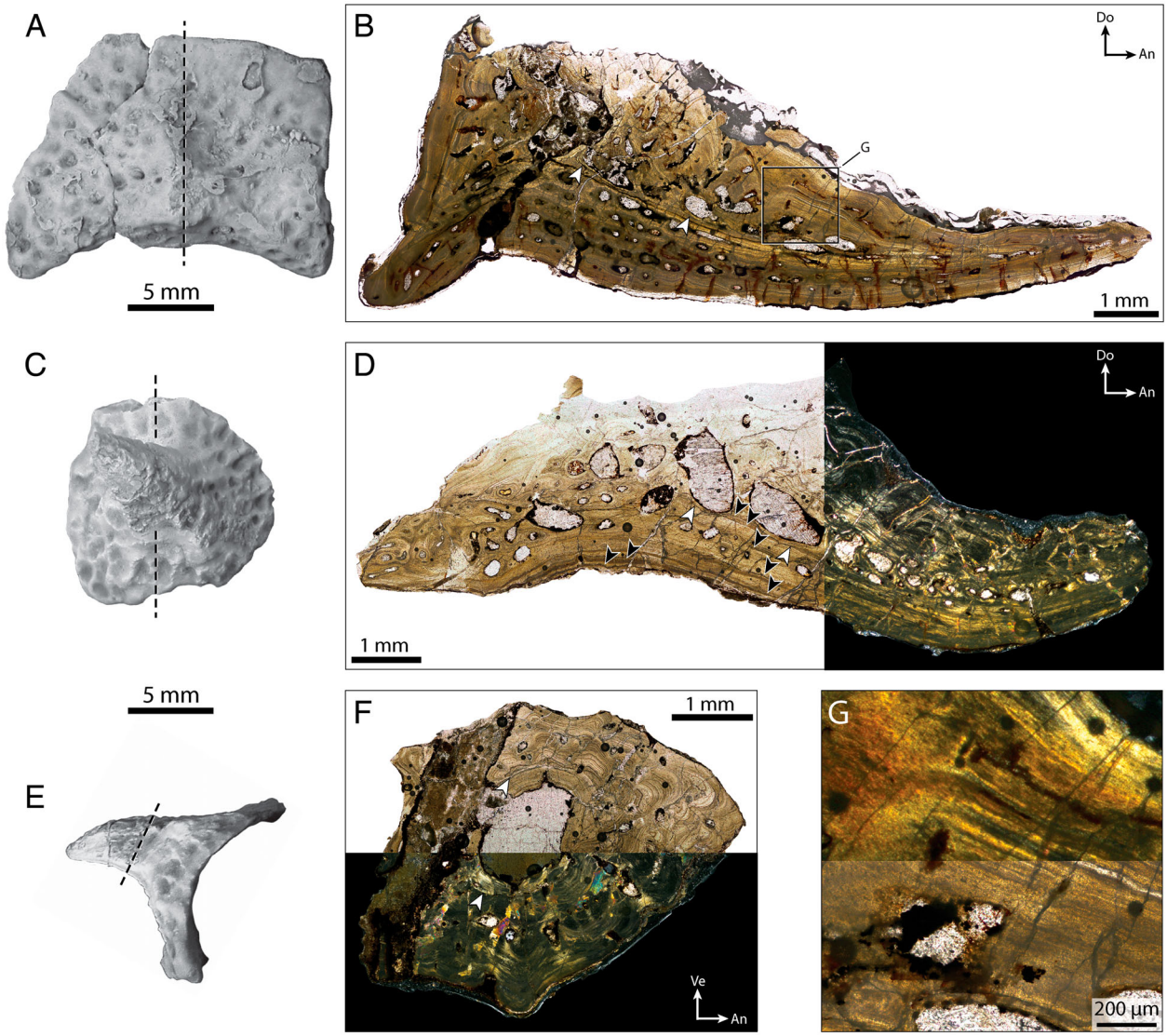

FIGURE 8. *Acaenasuchus geoffreyi*, osteoderm bone histology. **A**, **B**, UCMP 175103, paramedian osteoderm in **A**, dorsal view and **B**, longitudinal section. **C**–**F**, UCMP 175114, lateral osteoderm in **C**, lateral view, **D**, longitudinal section, **E**, posterior view, and **F**, transverse section. **G**, close-up image of the area of UCMP 175103 indicated by the box in **B**. Dashed lines in **A**, **C**, and **E** indicate plane of histological section. Black arrows in **D** and **F** indicate growth marks and white arrows in **B**, **D**, and **F** indicate areas of resorption with subsequent deposition of secondary bone tissue. Histological photographs (**B**, **D**, **F**, **G**) with white backgrounds are imaged in plane light, and those with black backgrounds are imaged in cross-polarized light. Surrounding epoxy has been cropped out for clarity; see Morphobank Project P3406 for original full-resolution histological images. Specimens were coated with ammonium chloride sublimate for clarity in full element photos (**A**, **C**, **E**). **Abbreviations**: **An**, anterior; **Do**, dorsal; **Ve**, ventral.

Acaenasuchus specimens. The three growth marks closest to the external surface of UCMP 175114 (Fig. 8D) are much closer together than the preceding internal marks, suggesting that skeletal growth is slowing. The anterior and posterior margins of the osteoderms, where bone appositional rate is greatest (Cerda and Desojo, 2011:fig. 5; Taborda et al., 2013:fig. 4; Cerda et al., 2018: fig. 9), lack the condition of dense longitudinal simple canals observed in juvenile stagonolepidid aetosaurs (Parker et al., 2008; R.B.I., pers. observ.). Though the sampled *Acaenasuchus* osteoderms possess relatively little internal cancellous bone compared to stagonlepidids, the larger endosteal spaces do show evidence of remodeling, with resorption lines external to secondary bone lining the circumference of each opening (Fig. 8B, D, F). This remodeling of endosteal vascular spaces is common in older archosaur osteoderms (e.g., de Buffrénil, 1982; Cerda and Desojo, 2011; Cerda et al., 2013, 2018; Scheyer et al., 2014). Thus, the balance of histological evidence suggests these osteoderms do not belong to a fast-growing young juvenile of a larger-bodied taxon (e.g., *Desmatosuchus*). Rather, they appear to be from a sub-adult ontogenetic stage where growth is beginning to slow. All of the *Acaenasuchus* material reported in this paper is within the same general size class as the sampled osteoderms, suggesting that our ontogenetic interpretations are representative for the sample.

PHYLOGENETIC ANALYSIS

We added 16 characters (nos. 420–435) from Parker (2016a) and ten novel characters (nos. 436–445) to the morphological character-taxon data matrix constructed by Nesbitt (2011) as modified by Butler et al. (2014) and Nesbitt et al. (2017). We also added additional states to five existing characters (422, 424,

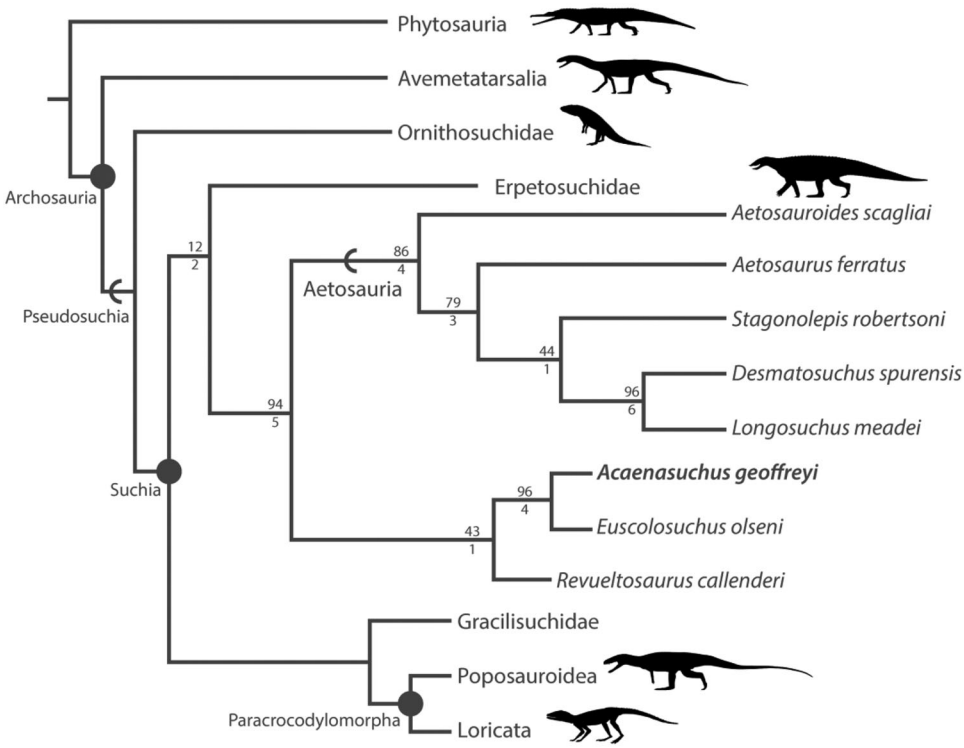

FIGURE 9. Strict consensus tree of the 227 MPTs (L = 1,414) resulting from the parsimony analysis of this study. Upper numbers represent bootstrap resampling values and lower numbers represent Bremer support values. Silhouettes modified from phylopic.org (see Acknowledgments).

427, 432, 408), rescored *Revueltosaurus callenderi* for select characters (171, 219, 268, 383, 406), rescored *Aetosaurus ferratus* for a character (375), and added *Desmatosuchus spurensis* and *Aetosauroides scagliai* to the matrix. We scored *Acaenasuchus geoffreyi* and *Euscolosuchus olseni* into the character-taxon matrix using Mesquite v3.10 (Maddison and Maddison, 2018) such that the final matrix includes 91 taxa and 445 characters (only the holotype specimens of *Teleocrater rhadinus*, *Poposaurus gracilis*, *Prestosuchus chiniquensis*, *Lewisuchus admixtus*, and *Asilisaurus kongwe* were used; Supplementary Data 3, 4; MorphoBank P3406). Characters 32, 52, 75, 121, 137, 139, 156, 168, 188, 223, 247, 258, 269, 271, 291, 297, 328, 356, 399, and 413 were ordered in the analysis (as they were in the parent data matrices), which was conducted using a heuristic tree search in TNT v1.5 (Goloboff et al., 2008) with 1,000 replications, random sequence addition, and tree bisection reconnection swapping while keeping ten trees per replication and condensing zero-length branches. A strict consensus tree was computed in TNT from all recovered most parsimonious trees (MPTs). Bootstrap resampling analyses were run using 1,000 replications with replacement. Parsimony-based ancestral state reconstruction was performed on the strict consensus tree using Mesquite to examine character state evolution.

The heuristic search recovered 227 MPTs with a length of 1,414 steps, a consistency index (CI) of 0.368, and a retention index (RI) of 0.769. The strict consensus tree of all MPTs (Fig. 9) recovers largely the same relationships as Nesbitt et al. (2017) and Butler et al. (2017) among non-archosaur archosauromorphs, avemetatarsalians, and non-aetosaurian suchians. Figure 9 displays an abbreviated version of the strict consensus tree (with larger clades collapsed into single branches for brevity) that also displays the GC bootstrap and Bremer values for each node. Within Pseudosuchia, Ornithosuchidae is the earliest diverging clade, and sister taxon to Suchia, in contrast with the topology recovered by Ezcurra et al. (2017) and Müller et al. (2020), in which ornithosuchids are the sister taxon of Erpetosuchidae and along with aetosaurs comprise a clade within Suchia (see von Baczko et al. [2020] for a synthesis of hypothesized ornithosuchid and erpetosuchid relationships within Pseudosuchia). Though poorly supported, our analysis recovers a monophyletic group of non-paracrocodylomorph suchians in which Erpetosuchidae (sensu Nesbitt and Butler, 2013) is the sister taxon to a well-supported clade that comprises *Revueltosaurus callenderi* Hunt, 1989, *Acaenasuchus geoffreyi* Long and Murry, 1995, *Euscolosuchus olseni* Sues, 1992, and Aetosauria (sensu Parker, 2007). The sister taxon to the stem-based group Aetosauria is the clade comprising *Revueltosaurus callenderi* + (*Acaenasuchus geoffreyi* + *Euscolosuchus olseni*) (Fig. 9). The representative aetosaur taxa in our analysis are recovered in the same relative position as found by Parker (2016a), with *Aetosauroides scagliai* as the most basal aetosaur. Enforcing the constraint of including ornithosuchids + erpetosuchids along with Aetosauria as a clade of suchians (sensu Ezcurra et al., 2017, Müller et al., 2020) requires an additional seven steps. Pulling *Revueltosaurus callenderi* just outside of the *Acaenasuchus geoffreyi* + *Euscolosuchus olseni* clade (making *Revueltosaurus callenderi* the sister taxon of Aetosauria, sensu Nesbitt, 2011 and Parker, 2016a) requires one additional step.

The clade *Acaenasuchus geoffreyi* + *Euscolosuchus olseni* is diagnosed by four unambiguous apomorphies: ornamented dorsal surface of the anterior bar of paramedian and lateral osteoderms; anteroposteriorly broadened transverse processes of trunk vertebrae; dorsal surface of neural arch of trunk vertebrae is nearly as mediolaterally wide and anteroposteriorly long; and anteroposteriorly broadened proximal ends of trunk ribs. The clade *Revueltosaurus callenderi* + (*Acaenasuchus geoffreyi* + *Euscolosuchus olseni*) is diagnosed by two unambiguous

apomorphies (although neither can be scored for *Euscolosuchus olseni*): frontal tapers anteriorly along the midline; presence of enlarged denticles on the maxillary teeth.

DISCUSSION

At the time when *Acaenasuchus geoffreyi* was first described by Long and Murry (1995), the phylogenetic relationships of Archosauriformes and Archosauria were only beginning to be elucidated using quantitative cladistic methods (e.g., Benton and Clark, 1988; Gauthier et al., 1988; Sereno, 1991; Parrish, 1993), and the only consensus was on the monophyly of major clades (e.g., Proterochampsia, Phytosauria, Aetosauria, Crocodylomorpha, Dinosauria). With a renaissance of Triassic research beginning in the early 2000s, new specimens helped to clarify these relationships, such as *Vancleavea campi* (Nesbitt et al., 2009), *Arizonasaurus babbitti* (Nesbitt, 2005), *Erpetosuchus granti* (Benton and Walker, 2002), *Revueltosaurus callenderi* (Parker et al., 2005), *Effigia okeefeae* (Nesbitt, 2007), and *Silesaurus opolensis* (Dzik, 2003). Other studies re-evaluated existing taxa and clarified particular aspects of early archosaur relationships (e.g., Ezcurra, 2006; Nesbitt et al., 2007; Irmis et al., 2007a, 2007b; Parker, 2007; Stocker, 2010; Brusatte et al., 2010) and led to a significant comprehensive revision of archosaurian phylogeny (Nesbitt, 2011), as well as early archosauriform and archosauromorph relationships (e.g., Ezcurra, 2016; Sookias, 2016; Pritchard and Sues, 2019). This work has provided the framework for a re-examination of many poorly understood Triassic taxa (e.g., Nesbitt et al., 2011; Stocker et al., 2016; Ezcurra et al., 2017; Butler et al., 2011, 2019a, 2019b), as well as spectacular new specimens that have further elucidated the relationships of early archosaurs and relatives (e.g., Nesbitt et al., 2012a, 2014, 2018a; Nesbitt and Butler, 2013; Pinheiro et al., 2016; Sengupta et al., 2017; Butler et al., 2018; Pritchard et al., 2018). Particularly relevant was the recognition that a number of enigmatic pseudosuchian taxa were early-diverging lineages at the base of Suchia (e.g., Nesbitt and Butler, 2013; Butler et al., 2014), and that taxa such as *Parringtonia*, *Erpetosuchus*, and *Revueltosaurus* might share a close relationship with aetosaurs (Nesbitt, 2011; Butler et al., 2014; Ezcurra et al., 2017; Nesbitt et al., 2018b). This new framework allows us to re-evaluate two poorly studied taxa, *Acaenasuchus geoffreyi* and *Euscolosuchus olseni*, and we recover them in a new clade that is the sister group to Aetosauria. Placed in context, these new data allow us to better understand the origin of aetosaurs and the assembly of their distinctive body plan (Nesbitt et al., 2012b).

Using our phylogenetic hypothesis (Fig. 9) as a framework to understand character transformations along the lineage leading to Aetosauria, we can reconstruct the evolution of the aetosaur body plan from more cursorial carnivorous pseudosuchian ancestors. The common ancestor of erpetosuchids and aetosaurs was still likely a small-bodied cursorial carnivore but possessed two paramedian rows of rectangular osteoderms with anastomosing ornamentation (Benton and Walker, 2002; Nesbitt and Butler, 2013; Nesbitt et al., 2018b; Ezcurra et al., 2017). The common ancestor of *Revueltosaurus callenderi* and aetosaurs evolved cervical and dorsal paramedian osteoderms that were mediolaterally wider than anteroposteriorly long as well as the presence of ventral osteoderms (Parker et al., 2005). This lineage also began to evolve a less carnivorous diet, as reflected in dental and jaw character states (e.g., un-curved teeth with enlarged denticles, shortened tooth row, dorsoventrally enlarged surangular; Parker et al., 2005). Other changes towards the aetosaurian condition included a laterally rotated squamosal, and a more robust forelimb, with an enlarged scapulacoracoid and a mediolaterally wide but proximodistally short humerus. The common ancestor of *Revueltosaurus callenderi* and aetosaurs also evolved one or more extensive rows of lateral osteoderms that articulate with the lateral edge of the paramedian osteoderms, enlarged transverse processes and dorsal ribs to support this expanded carapace, a dorsoventrally taller but anteroposteriorly shorter ilium, and more robust hind limb elements. To the exclusion of *Revueltosaurus callenderi* and its closest relatives (*Acaenasuchus geoffreyi* and *Euscolosuchus olseni*), aetosaurs further modified the feeding apparatus by losing teeth in the anterior portion of the dentary and modifying the snout and dentary into distinct shapes (Desojo et al., 2013). Given the presence of ankylothecodonty in ornithodirans and non-archosaur archosauromorphs, and now in *Acaenasuchus geoffreyi*, an early diverging pseudosuchian, it suggests that either ankylothecodonty is ancestral for archosaurs and later lost independently in both pseudosuchians and ornithodirans, or gomphosis is ancestral for Archosauria and ankylothecodonty is regained independently in lineages such as silesaurids and *Acaenasuchus geoffreyi.* We note that *Revueltosaurus callenderi* (e.g., PEFO 34561) also exhibits ankylothecodont tooth implantation, possibly demonstrating this as a plesiomorphic state for the clade (*Revueltosaurus callenderi* (*Euscolosuchus olseni* + *Acaenasuchus geoffreyi*)).

The recognition that the rectangular ornamented osteoderms that characterized aetosaurs are also found outside of this clade calls into question the ability to use this type of osteoderm to assign fossils that consist of only isolated osteoderms to the Aetosauria. This was already suspected to some degree because aetosaur-like osteoderms are known from *Revueltosaurus callenderi* (Parker et al., 2005) and is supported further with the determination of *Acaenasuchus geoffreyi* and *Euscolosuchus olseni* as non-aetosaur suchians. Thus, isolated osteoderms with character states like the presence of an anterior bar from Upper Triassic deposits are best assigned only to Suchia, unless they possess the unambiguous synapomorphies or unique combination of character states of a known aetosaur taxon (see Parker, 2016a and the references therein). The same recommendation applies to isolated lateral osteoderms, as well. Even though the ornamented anterior bars of non-stagonolepidid aetosaurs could help differentiate them from stagonolepidids, this ornamentation is sometimes lost through erosion (e.g., the holotype specimen of *Acaenasuchus geoffreyi*, UCMP 139576; Fig. 2A).

In the cases of both *Revueltosaurus callenderi* and *Acaenasuchus geoffreyi* it is also important to note that the material was thought to belong to juvenile specimens of previously known taxa (Long and Ballew, 1985; Heckert and Lucas, 2002a, 2002b). These identifications had been contested (e.g., Irmis, 2005; Parker, 2005a, 2008) based on apomorphies of the osteoderms; however, it required the discovery of associated non-osteoderm remains to provide a final conclusion (Parker et al., 2005; this study), especially when all of the taxa are recovered as disarticulated elements in the same deposits (Heckert and Lucas, 2002a). Histological evidence has since supported the presence of a number of juvenile aetosaur specimens, including those of *Aetosauroides scagliai* (e.g., MCP 13; Taborda et al., 2013), *Aetosaurus ferratus* (e.g., SMNS 5770-S16; Taborda et al., 2013), and *Coahomasuchus chathamensis* (e.g., NCSM 23618; Hoffman et al., 2019).

Other than the overall morphology of the osteoderms, the character states primarily used to identify *Acaenasuchus geoffreyi* as a juvenile of *Desmatosuchus spurensis* were the presence of thickened 'tongue-and-groove' lateral and medial articulation surfaces with adjacent osteoderms, and the presence of a depressed anterior lamina rather than a raised anterior 'bar' (both characters following the definition of Long and Ballew, 1985). An 'anterior lamina' was only observed in the holotype specimen whereas all referred *Acaenasuchus geoffreyi* specimens have a clearly raised anterior bar, and we can now demonstrate the holotype is badly weathered and the beveled anterior surface is an alteration from this weathering and over-

preparation. The interdigitating 'tongue and groove' articulations appear to be a convergence with desmatosuchine stagonolepidids; however, they are also fundamentally different between *Acaenasuchus geoffreyi* and *Desmatosuchus spurensis*. In both lineages the surfaces are dorsoventrally thickened relative to the rest of the osteoderm, but in *Acaenasuchus geoffreyi* the lateral and medial faces are often vertical and flat, whereas in *Desmatosuchus spurensis* they are very complex with more elongate lateral projections and deeper hollows creating a more interlocking suture. Furthermore, in *Desmatosuchus spurensis* these articulation surfaces are only observed in the cervical and anterior trunk regions (Parker, 2005b, 2008), whereas in *Acaenasuchus geoffreyi* they occur throughout the carapace. In addition, *Acaenasuchus geoffreyi* also possesses sets of anterior and posterior articular surfaces differing significantly from what is present in aetosaurs. In fact, it was recognition of these different sutural patterns in the osteoderms that originally led to the hypothesis that *Acaenasuchus geoffreyi* was not a stagonolepidid aetosaur, supported by subsequent discovery of associated non-osteoderm material.

Recent work is refining our understanding of the phylogenetic relationships among early archosaurian groups (e.g., Butler et al., 2014; Stocker et al., 2016; Nesbitt et al., 2017), further emphasizing the importance of apomorphy-based identifications in vertebrate paleontology (e.g., Nesbitt and Stocker, 2008; Lessner et al., 2018; Pritchard and Sues, 2019). Because different skeletal modules (e.g., cranium, carapace) can possess conflicting phylogenetic signals (see discussion in Parker, 2016a), taxa known from only a single module can act as wildcard taxa in a phylogenetic analysis (e.g., Kearney and Clark, 2003) grouping with taxa with similar modules. For example, when *Acaenasuchus geoffreyi* is scored for only osteoderm characters, it is recovered within the clade Stagonolepididae (e.g., Parker, 2007, 2016a; Parker et al., 2008; Desojo et al., 2012; Heckert et al., 2015). Pritchard and Sues (2019) recently discussed this phenomenon in regard to the archosauromorph *Teraterpeton hrynewichorum*. If *Teraterpeton* is scored for character states observed in the ilium it would be recovered as a rhynchosaurian, and the fifth metatarsal as a tanystropheid; however, a total evidence scoring from a relatively complete specimen provides its current placement within Allokotosauria (Pritchard and Sues, 2019). Thus, new fossils and character state determinations can stabilize these wild card taxa, allowing them to contribute more fully to analyses. In the present case the discovery of additional material of *Acaenasuchus geoffreyi* clarifies the relationships of that taxon as a member of a newly recognized sister clade of aetosaurs that includes the pseudosuchians *Revueltosaurus callenderi* and *Euscolosuchus olseni*.

CONCLUSIONS

The relationships of *Acaenasuchus geoffreyi* and its taxonomic validity have long been debated due to a lack of non-osteoderm anatomical data and an evaluation of its ontogenetic stage. Our study uses cranial and non-osteoderm postcranial elements as well as osteohistological analysis to revise the skeletal anatomy of *Acaenasuchus geoffreyi*, better constrain its ontogeny status, and demonstrate that it is a valid small-bodied taxon belonging to a clade that is the sister taxon to Aetosauria. The analysis of non-osteoderm skeletal modules stabilizes the phylogenetic relationships of *Acaenasuchus geoffreyi*, and our inclusion of newly coded characters for *Revueltosaurus callenderi* and *Euscolosuchus olseni* recovers a close relationship to *Acaenasuchus* and aetosaurs. Our analysis of pseudosuchian relationships shows that erpetosuchids, *Revueltosaurus callenderi*, *Acaenasuchus geoffreyi*, *Euscolosuchus olseni*, and aetosaurs form a monophyletic clade diverse in diet, body size, and osteoderm morphology. The recognition of a new clade of non-aetosaurian armored suchians forms the phylogenetic framework for future studies in the temporal, biogeographic, and trophic evolution of this clade during the Late Triassic Epoch and provide new insights into the evolution of the aetosaur body plan.

ACKNOWLEDGMENTS

We thank D. and J. Gillette (MNA), P. Holroyd (UCMP), and C. Levitt-Bussian (UMNH) for providing collections and archive access, and for facilitating loans from their institutions. M. Polcyn (SMU) graciously sent us locality information and photographs of SMU 75403. H.-D. Sues provided photographs of and helpful comments on *Euscolosuchus olseni*, and J. Strotman facilitated the molding, casting, and transfer of casts of USNM 448587 and USNM 448582. P. Holroyd (UCMP) graciously provided permission to histologically section two osteoderms, and A. Lee (Midwestern University) kindly assisted with sectioning. K. Ritterbush (University of Utah) generously provided access to her petrographic microscope imaging system, and the histological slides were imaged by N. Ong. R. Long's field notes are on file in the archives at PEFO and the UCMP and those of Charles Camp are available at the UCMP. Thanks to T. Olson for finding MDM specimens at PFV 211. We thank J. Kirkland and D. DeBlieux (Utah Geological Survey) for permission to include in this study material they collected. The collection and preparation of the specimens from PEFO was funded by the Petrified Forest Museum Association and Friends of Petrified Forest National Park. Silhouettes from phylopic.org in Figure 9 were created by S. Hartman, D. Bogdanov, and Smokeybjb and reused under the Creative Commons Attribution 3.0 Unported license (creativecommons.org/licenses/by/3.0). Thanks to V. Paes Neto and D. Gillette for constructive comments and discussion on aetosaur and glyptodont anatomy, and to A. Turner for help in constraining tree topology in TNT. Comments and suggestions made by M. B. von Baczko and I. Cerda improved the manuscript. This is Petrified Forest National Park Contribution No. 61. The conclusions presented here are those of the authors and do not represent the views of the United States Government.

ORCID

Adam D. Marsh http://orcid.org/0000-0002-3223-8940
William G. Parker http://orcid.org/0000-0002-6005-7098
Ben T. Kligman http://orcid.org/0000-0003-4400-8963

LITERATURE CITED

Agnolín, F. L., and S. Rozadilla. 2018. Phylogenetic reassessment of *Pisanosaurus mertii* Casamiquela, 1967, a basal dinosauriform from the Late Triassic of Argentina. Journal of Systematic Palaeontology 16:853–879.

Arbour, V. M., and L. E. Zanno. 2018. The evolution of tail weaponization in amniotes. Proceedings of the Royal Society of London, Biological Sciences 285:20172299.

Atchley, S. C., L. C. Nordt, S. I. Dworkin, J. Ramezani, W. G. Parker, S. R. Ash, and S. A. Bowring. 2013. A linkage among Pangean tectonism, cyclic alluviation, climate change, and a biologic turnover in the Late Triassic: the record from the Chinle Formation, southwestern United States. Journal of Sedimentary Research 83:1147–1161.

Baczko, M. B. von, J. B. Desojo, and D. Ponce. 2020. Postcranial anatomy and osteoderm histology of Riojasuchus tenuisceps and a phylogenetic update on Ornthosuchidae (Archosauria, Pseudosuchia). Journal of Vertebrate Paleontology 39:e1693396.

Barendregt, R. W., and E. D. Ongley. 1977. Piping in the Milk River Canyon, southeastern Alberta - a contemporary dryland geomorphic process. Matter Transport in Inland Waters Symposium, IAHS-AISH Publication 122:233–243.

Benton, M. J. 1984. Tooth form, growth, and function in Triassic rhynchosaurs (Reptilia, Diapsida). Palaeontology 27:737–776.

Benton, M. J., and J. M. Clark. 1988. Archosaur phylogeny and the relationships of the Crocodylia; pp. 295–338 in M. J. Benton (ed.),

The Phylogeny and Classification of the Tetrapods, Volume 1: Amphibians, Reptiles, Birds. Clarendon Press, Oxford.
Benton, M. J., and A. D. Walker. 2002. *Erpetosuchus*, a crocodile-like basal archosaur from the Late Triassic of Elgin, Scotland. Zoological Journal of the Linnean Society 136:25–47.
Bertin, T. J., B. Thivichon-Prince, A. R. LeBlanc, M. W. Caldwell, and L. Viriot. 2018. Current perspectives on tooth implantation, attachment, and replacement in Amniota. Frontiers in Physiology 9:1–20.
Botha-Brink, J., and K. D. Angielczyk. 2010. Do extraordinarily high growth rates in Permo-Triassic dicynodonts (Therapsida, Anomodontia) explain their success before and after the end-Permian extinction? Zoological Journal of the Linnean Society 160:341–365.
Brochu, C. A. 1996. Closure of neurocentral sutures during crocodilian ontogeny: implications for maturity assessment in fossil archosaurs. Journal of Vertebrate Paleontology 16:49–62.
Brochu, C. A. 1997. A review of "*Leidyosuchus*" (Crocodyliformes, Eusuchia) from the Cretaceous through Eocene of North America. Journal of Vertebrate Paleontology 17:679–697.
Brusatte, S. L., M. J. Benton, J. B. Desojo, and M. C. Langer. 2010. The higher-level phylogeny of Archosauria (Tetrapoda: Diapsida). Journal of Systematic Palaeontology 8:3–47.
Brust, A. C. B., J. B. Desojo, C. L. Schultz, V. D. Paes-Neto, and A. A. S. Da-Rosa. 2018. Osteology of the first skull of *Aetosauroides scagliai* Casamiquela 1960 (Archosauria: Aetosauria) from the Upper Triassic of southern Brazil (*Hyperodapedon* Assemblage Zone) and its phylogenetic importance. PLoS One 13:e0201450.
Butler, R. J., S. L. Brusatte, M. Reich, S. J. Nesbitt, R. R. Schoch, and J. J. Hornung. 2011. The sail-backed reptile *Ctenosauriscus* from the latest Early Triassic of Germany and the timing and biogeography of the early archosaur radiation. PLoS One 6:e25693.
Butler, R. J., C. Sullivan, M. D. Ezcurra, J. Liu, A. Lecuona, and R. B. Sookias. 2014. New clade of enigmatic early archosaurs yields insights into early pseudosuchian phylogeny and the biogeography of the archosaur radiation. BMC Evolutionary Biology 14:128.
Butler, R. J., S. J., Nesbitt, A. J., Charig, D. J. Gower, and P. M. Barrett. 2018. *Mandasuchus tanyauchen*, gen. et sp. nov., a pseudosuchian archosaur from the Manda Beds (?Middle Triassic) of Tanzania. Society of Vertebrate Paleontology Memoir 17:96–121.
Butler, R. J., M. D. Ezcurra, J. Liu, R. B. Sookias, and C. Sullivan. 2019. The anatomy and phylogenetic position of the erythrosuchid archosauriform *Guchengosuchus shiguaiensis* from the earliest Middle Triassic of China. PeerJ 7:e6435.
Butler, R. J., A. G. Sennikov, E. M. Dunne, M. D. Ezcurra, B. P. Hedrick, S. C. R. Maidment, L. E. Meade, T. J. Raven, and D. J. Gower. 2019. Cranial anatomy and taxonomy of the erythrosuchid archosauriform '*Vjushkovia triplicostata*' Huene, 1960, from the Early Triassic of European Russia. Royal Society Open Science 6:191289.
Camp, C. L. 1924. Unpublished field notes.
Camp, C. L., and G. D. Hanna. 1937. Methods in Paleontology. University of California Press, Berkeley, 153 pp.
Campione, N. E., K. S. Brink, E. A. Freedman, C. T. McGarrity, and D. C. Evans. 2013. '*Glishades ericksoni*', an indeterminate juvenile hadrosaurid from the Two Medicine Formation of Montana: implications for hadrosauroid diversity in the latest Cretaceous (Campanian-Maastrichtian) of western North America. Palaeobiodiversity and Palaeoenvironments 93:65–75.
Carlini, A. A., A. E. Zurita, and O. Aguilera. 2008. North American glyptodontines (Xenarthra, Mammalia) in the Upper Pleistocene of northern South America. Paläontologische Zeitschrift 82:125–138.
Carroll, P. H. 1949. Soil piping in southeastern Arizona. Soil Conservation Service Regional Bulletin 110:1–21.
Case, T. J. 1978. On the evolution and adaptive significance of postnatal growth rates in the terrestrial vertebrates. Quarterly Review of Biology 53:243–282.
Cerda, I. A., and J. B. Desojo. 2011. Dermal armour histology of aetosaurs (Archosauria: Pseudosuchia), from the Upper Triassic of Argentina and Brazil. Lethaia 44:417–428.
Cerda, I. A., J. B. Desojo, T. M. Scheyer, and C. L. Schultz. 2013. Osteoderm microstructure of 'rauisuchian' archosaurs from South America. Geobios 46:273–283.
Cerda, I. A., J. B. Desojo, and T. M. Scheyer. 2018. Novel data on aetosaur (Archosauria, Pseudosuchia) osteoderm microanatomy and histology: palaeobiological implications. Palaeontology 61:721–745.
Chatterjee, S. 1974. A rhynchosaur from the Upper Triassic Maleri formation of India. Philosophical Transactions of the Royal Society of London B, Biological Sciences 267:209–261.
Chiasson, R. B. 1962. Laboratory Anatomy of the Alligator. W. C. Borown Company Publishers, Dubuque, Iowa, 56 pp.
Clarke, J. A., and K. M. Middleton. 2008. Mosaicism, modules, and the evolution of birds: results from a Bayesian approach to the study of morphological evolution using discrete character data. Systematic Biology 57:185–201.
Colbert, E. H., and C. C. Mook. 1951. The ancestral crocodilian *Protosuchus*. Bulletin of the American Museum of Natural History 97:143–182.
Cope, E. D. 1869. Synopsis of the extinct Batrachia, Reptilia and Aves of North America. Transactions of the American Philosophical Society 14:1–252.
Cubo, J., P. Legendre, A. de Ricqlès, L. Montes, E. de Margerie, J. Castanet, and Y. Desdevises. 2008. Phylogenetic, functional, and structural components of variation in bone growth rate of amniotes. Evolution & Development 10:217–227.
Currey, J. D., and R. M. Alexander. 1985. The thickness of the walls of tubular bones. Journal of Zoology 206:453–468.
de Beer, G. R. 1954. *Archaeopteryx lithographica*: a study based upon the British Museum specimen. British Museum of Natural History, London.
de Buffrénil, V. 1982. Morphogenesis of bone ornamentation in extant and extinct crocodilians. Zoomorphology 99:155–166.
de Margerie, E., J. Cubo, and J. Castanet. 2002. Bone typology and growth rate: testing and quantifying 'Amprino's rule' in the mallard (*Anas platyrhynchos*). Comptes Rendus Biologies 325:221–230.
de Margerie, E., J.-P. Robin, D. Verrier, J. Cubo, R. Groscolas, and J. Castanet. 2004. Assessing a relationship between bone microstructure and growth rate: a fluorescent labelling study in the king penguin chick (*Aptenodytes patagonicus*). Journal of Experimental Biology 207:869–879.
Desojo, J. B. and A. M. Báez. 2005. El esqueleto postcraneano de *Neoaetosauroides* (Archosauria: Aetosauria) del Triásico Superior del centro-oeste de Argentina. Ameghiniana 42:115–126.
Desojo, J. B., and S. F. Vizcaíno. 2009. Jaw biomechanics in the South American aetosaur *Neoaetosauroides engaenus*. Paläeontologische Zeitschrift 83:499–510.
Desojo, J. B., M. D. Ezcurra, and E. E. Kischlat. 2012. A new aetosaur genus (Archosauria: Pseudosuchia) from the early Late Triassic of southern Brazil. Zootaxa 3166:1–33.
Desojo, J. B., A. B. Heckert, J. W. Martz, W. G. Parker, R. R. Schoch, B. J. Small, and T. Sulej. 2013. Aetosauria: a clade of armoured pseudosuchians from the Upper Triassic continental beds. Geological Society of London Special Publication 379:203–239.
Dilkes, D., and H.-D. Sues. 2009. Redescription and phylogenetic relationships of *Doswellia kaltenbachi* (Diapsida: Archosauriformes) from the Upper Triassic of Virginia. Journal of Vertebrate Paleontology 29:58–79.
Donoghue, M. J., J. A. Doyle, J. Gauthier, A. G. Kluge, and T. Rowe. 1989. The importance of fossils in phylogeny reconstruction. Annual Review of Ecology and Systematics 20:431–460.
Dubiel, R. F. 1987. Sedimentology and new fossil occurrences of the Upper Triassic Chinle Formation, southeastern Utah. Four Corners Geological Society Guidebook 10:99–107.
Dzik, J. 2003. A beaked herbivorous archosaur with dinosaur affinities from the early Late Triassic of Poland. Journal of Vertebrate Paleontology 23:556–574.
Erickson, G. M., and C. A. Brochu. 1999. How the 'terror crocodile' grew so big. Nature 398:205–206.
Estep, J. W., A. B. Heckert, and S. G. Lucas. 1998. *Acaenasuchus geoffreyi* (Archosauria: Aetosauria) from the Upper Triassic Chinle Group: juvenile of *Desmatosuchus haplocerus*. Journal of Vertebrate Paleontology 18(3, Supplement):40A.
Ezcurra, M. D. 2006. A review of the systematic position of the dinosauriform archosaur *Eucoelophysis baldwini* Sullivan & Lucas, 1999 from the Upper Triassic of New Mexico, USA. Geodiversitas 28:649–684.
Ezcurra, M. D. 2016. The phylogenetic relationships of basal archosauromorphs, with an emphasis on the systematics of proterosuchian archosauriforms. PeerJ 4:e1778.
Ezcurra, M. D., L. E. Fiorelli, A. G. Martinelli, S. Rocher, M. B. von Baczko, M. Ezpeleta, J. R. A. Taborda, E. M. Hechenleitner, M. J. Trotteyn, and J. B. Desojo. 2017. Deep faunistic turnovers preceded

the rise of dinosaurs in southwestern Pangaea. Nature Ecology and Evolution 1:1477–1483.
Fink, W. L. 1981. Ontogeny and phylogeny of tooth attachment modes in actinopterygian fishes. Journal of Morphology 167:167–184.
Francillon-Vieillot, H., V. de Buffrénil, J. Castanet, J. Géraudie, F. J. Meunier, J. Y. Sire, L. Zylberberg, and A. de Ricqlès. 1990. Microstructure and mineralization of vertebrate skeletal tissues; pp. 471–671 in J. G. Carter (ed.), Skeletal Biomineralization: Patterns, Processes and Evolutionary Trends, Volume I. Van Nostrand Reinhold, New York.
Gaffney, E. S. 1985. The cervical and caudal vertebrae of the cryptodiran turtle, *Meiolania platyceps*, from the Pleistocene of Lord Howe Island, Australia. American Museum Novitates 2805:1–29.
Gaffney, E. S. 1990. The comparative osteology of the Triassic turtle *Proganochelys*. Bulletin of the American Museum of Natural History 194:1–263.
Games, I. 1990. Growth curves for the Nile crocodile as estimated by skeletochronology; pp. 111–121 in Crocodiles: Proceedings of the 10th Working Meeting of the Crocodile Specialist Group, Volume 1. IUCN - The World Conservation Union, Gland, Switzerland.
Gauthier, J., A. G. Kluge, and T. Rowe. 1988. Amniote phylogeny and the importance of fossils. Cladistics 4:105–209.
Gee, B. M. 2020. Size matters: the effects of ontogenetic disparity on the phylogeny of Trematopidae (Amphibia: Temnospondyli). Zoological Journal of the Linnean Society. doi: 10.1093/zoolinnean/zlz170.
Goloboff, P. A., J. S. Farris, and K. C. Nixon. 2008. TNT, a free program for phylogenetic analysis. Cladistics 24:774–786.
Gower, D. J. 2003. Osteology of the early archosaurian reptile *Erythrosuchus africanus* Broom. Annals of the South African Museum 110:1–84.
Gower, D. J., and R. Schoch. 2009. Postcranial anatomy of the rauisuchian archosaur *Batrachotomus kupferzellensis*. Journal of Vertebrate Paleontology 29:103–122.
Griffin, C. T. 2018. Developmental patterns and variation among early theropods. Journal of Anatomy 232:604–640.
Harris, S. R., D. J. Gower, and M. Wilkinson. 2003. Phylogenetic methods and aetosaur interrelationships: a rejoinder. Systematic Biology 52:851–852.
Heckert, A. B. 2002. A revision of the Upper Triassic ornithischian dinosaur *Revueltosaurus*, with a description of a new species. New Mexico Museum of Natural History and Science Bulletin 21:253–266.
Heckert, A. B. 2004. Late Triassic microvertebrates from the Upper Triassic Chinle Group (Otischalkian-Adamanian: Carnian), southwestern U.S.A. New Mexico Museum of Natural History and Science Bulletin 27:1–170.
Heckert, A. B., and S. G. Lucas. 1999. A new aetosaur (Reptila: Archosauria) from the Upper Triassic of Texas and the phylogeny of aetosaurs. Journal of Vertebrate Paleontology 19:50–68.
Heckert, A. B., and S. G. Lucas. 2000. Taxonomy, phylogeny, biostratigraphy, biochronoogy, paleobiogeography, and the evolution of the Late Triassic Aetosauria (Archosauria: Crurotarsi). Zentralblatt für Geologie und Paläontologie, Teil I 1998:1539–1587.
Heckert, A. B. and S. G. Lucas. 2002a. *Acaenasuchus geoffreyi* (Archosauria: Aetosauria) from the Upper Triassic Chinle Group: juvenile of *Desmatosuchus haplocerus*. New Mexico Museum of Natural History and Science Bulletin 21:205–214.
Heckert, A. B., and S. G. Lucas. 2002b. Osteoderms of juveniles of *Stagonolepis* (Archosauria: Aetosauria) from the lower Chinle Group, east-central Arizona. New Mexico Museum of Natural History and Science Bulletin 21:235–239.
Heckert, A. B., S. G. Lucas, L. F. Rinehart, M. D. Celeskey, J. A. Spielmann, and A. P. Hunt. 2010. Articulated skeletons of the aetosaur *Typothorax coccinarum* Cope (Archosauria: Stagonolepididae) from the Upper Triassic Bull Canyon Formation (Revueltian: early-mid Norian), eastern New Mexico, USA. Journal of Vertebrate Paleontology 30:619–642.
Heckert, A. B., S. G. Lucas, and J. A. Spielmann. 2012. A new species of the enigmatic archosauromorph *Doswellia* from the Upper Triassic Bluewater Creek Formation, New Mexico, USA. Palaeontology 55:1333–1348.
Heckert, A. B., V. P. Schneider, N. C. Fraser, and R. A. Webb. 2015. A new aetosaur (Archosauria: Suchia) from the Upper Triassic Pekin Formation, Deep River Basin, North Carolina, U.S.A., and its implications for early aetosaur evolution. Journal of Vertebrate Paleontology 35:e3881831.
Hoffmann, D. K., A. B. Heckert, and L. E. Zanno. 2019. Disparate growth strategies within Aetosauria: novel histologic data from the aetosaur *Coahomasuchus chathamensis*. The Anatomical Record 302:1504–1515.
Hua, S., and V. de Buffrénil. 1996. Bone histology as a clue in the interpretation of functional adaptations in the Thalattosuchia (Reptilia, Crocodylia). Journal of Vertebrate Paleontology 16:703–717.
Hunt, A. P. 1989. A new ?ornithischian dinosaur from the Bull Canyon Formation (Upper Triassic) of east-central New Mexico; pp. 355–358 in S. G. Lucas and A. P. Hunt (eds.), Dawn of the Age of Dinosaurs in the American Southwest. New Mexico Museum of Natural History and Science, Albuquerque, New Mexico.
Hunt, A. P. 1998. Preliminary results of the Dawn of the Dinosaur Project at Petrified Forest National Park, Arizona; pp. 135–137 in V. L. Santucci and L. McClelland (eds.), National Park Service Paleontological Research Volume 1, Geological Resources Division Technical Report NPS/NRGRD/GRDTR-98/01. United States Department of the Interior, Washington, D.C.
Hunt, A. B., and J. Wright. 1999. New discoveries of Late Triassic dinosaurs from Petrified Forest National Park, Arizona; pp. 96–100 in V. L. Santucci and L. McClelland (eds.), National Park Service Paleontological Research Volume 4, Geological Resources Division Technical Report NPS/NRGRD/GRDTR-99/03. United States Department of the Interior, Washington, D.C.
Hutton, J. M. 1986. Age determination of living Nile crocodiles from the cortical stratification of bone. Copeia 1986:332–341.
Irmis, R. B. 2005. The vertebrate fauna of the Upper Triassic Chinle Formation in northern Arizona. Mesa Southwest Museum Bulletin 9:63–88.
Irmis, R. B. 2007. Axial skeleton ontogeny in the Parasuchia (Archosauria: Pseudosuchia) and its implications for ontogenetic determination in archosaurs. Journal of Vertebrate Paleontology 27:350–361.
Irmis, R. B., W. G. Parker, S. J. Nesbitt, and J. Liu. 2007a. Early ornithischian dinosaurs: the Triassic record. Historical Biology 19:3–22.
Irmis, R. B., S. J. Nesbitt, K. Padian, N. D. Smith, A. H. Turner, D. T. Woody, and A. Downs. 2007b. A Late Triassic dinosauromorph assemblage from New Mexico and the rise of dinosaurs. Science 317:358–361.
Jacobs, L. L., and P. A. Murry. 1980. The vertebrate community of the Triassic Chinle Formation near St. Johns, Arizona; pp. 55–71 in L. L. Jacobs (ed.), Aspects of Vertebrate History: Essays in Honor of Edwin Harris Colbert. Museum of Northern Arizona Press, Flagstaff.
Jones, A. 1971. Soil piping and stream channel initiation. Water Resources Research 7:601–610.
Kaye, F. T., and K. Padian. 1994. Microvertebrates from the Placerias Quarry: a window on Late Triassic vertebrate diversity in the American Southwest; pp. 171–196 in N. C. Fraser and H.-D. Sues (eds.), In the Shadow of the Dinosaurs: Early Mesozoic Tetrapods. Cambridge University Press, Cambridge.
Kammerer, C. F., S. J. Nesbitt, and N. H. Shubin. 2011. The first silesaurid dinosauriform from the Late Triassic of Morocco. Acta Palaeontologica Polonica 57:277–284.
Kearney, M. 2002. Fragmentary taxa, missing data, and ambiguity: mistaken assumptions and conclusions. Systematic Biology 51:369–381.
Kearney, M., and J. M. Clark. 2003. Problems due to missing data in phylogenetic analyses including fossils: a critical review. Journal of Vertebrate Paleontology 23:263–274.
Keeble, E., and M. J. Benton. 2020. Three-dimensional tomographic study of dermal armour from the tail of the Triassic aetosaur *Stagonolepis robertsoni*. Scottish Journal of Geology 56:55–62.
Kent, D. V., P. E. Olsen, C. Rasmussen, C. Lepre, R. Mundil, R. B. Irmis, G. E. Gehrels, D. Giesler, J. W. Geissman, and W. G. Parker. 2018. Empirical evidence for stability of the 405-kiloyear Jupiter-Venus eccentricity cycle over hundreds of millions of years. Proceedings of the National Academy of Sciences 115:6153–6158.
Kent, D. V., P. E. Olsen, C. Lepre, C. Rasmussen, R. Mundil, G. E. Gehrels, D. Giesler, R. B. Irmis, J. W. Geissman, and W. G. Parker. 2019. Magnetochronology of the entire Chinle Formation (Norian age) in a scientific drill core from Petrified Forest National Park (Arizona, USA) and implications for regional and global correlations in the Late Triassic. Geochemistry, Geophysics, Geosystems 20:1–8.
Kischlat, E. E. 2000. Tecodoncios: a aurora dos arcossáurios Triássico; pp. 273–316 in M. Holz and L. F. de Ros (eds.), Paleontologia do Rio Grande do Sul. Edição CIGO/UFRGS, Port Allegre, Brazil.

Kligman, B. T., W. G. Parker, and A. D. Marsh. 2017. First record of *Saurichthys* (Actinopterygii) from the Upper Triassic (Chinle Formation, Norian) of western North America. Journal of Vertebrate Paleontology 37:e1367304.

Kligman, B. T., A. D. Marsh, and W. G. Parker. 2018. First records of diapsid *Palacrodon* from the Norian, Late Triassic Chinle Formation of Arizona, and their biogeographic implications. Acta Palaeontologica Polonica 63:117–127.

Krebs, B. 1974. Die Archosaurier. Naturwissenschaften 61:17–24.

Lacerda, M. B., M. A. G. de França, and C. L. Schultz. 2018. A new erpetosuchid (Pseudosuchia, Archosauria) from the Middle–Late Triassic of southern Brazil. Zoological Journal of the Linnean Society 184:804–824.

Lamm, E.-T. 2013. Preparation and sectioning of specimens; pp. 55–160 in K. Padian and E.-T. Lamm (eds.), Bone Histology of Fossil Tetrapods: Advancing Methods, Analysis, and Interpretation. University of California Press, Berkeley.

Langer, M. C., and J. Ferigolo. 2013. The Late Triassic dinosauromorph *Sacisaurus agudoensis* (Caturrita Formation; Rio Grande do Sul, Brazil): anatomy and affinities. Geological Society of London Special Publication 379:353–392.

Langer, M. C., M. A. G. Franca, and S. Gabriel. 2007. The pectoral girdle and forelimb anatomy of the stem-sauropodomorph *Saturnalia tupiniquim* (Upper Triassic, Brazil). Special Papers in Palaeontology 77:113–137.

Langer, M. C., S. J. Nesbitt, J. S. Bittencourt, and R. B. Irmis. 2013. Non-dinosaurian Dinosauromorpha. Geological Society of London Special Publications 379:157–186.

LeBlanc, A. R., K. S. Brink, T. M. Cullen, and R. R. Reisz. 2017. Evolutionary implications of tooth attachment versus tooth implantation: a case study using dinosaur, crocodilian, and mammal teeth. Journal of Vertebrate Paleontology 37:e1354006.

Lessner, E. J., W. G. Parker, A. D. Marsh, S. J. Nesbitt, R. B. Irmiss, and B. D. Mueller. 2018. New insights into Late Triassic dinosauromorph-bearing assemblages from Texas using apomorphy-based identifications. PaleoBios 35:1–41.

Long, R. A., and K. L. Ballew. 1985. Aetosaur dermal armor from the Late Triassic of southwestern North America, with special reference to material from the Chinle Formation of Petrified Forest National Park. Museum of Northern Arizona Bulletin 47:45–68.

Long, R. A., and P. A. Murry. 1995. Late Triassic (Carnian and Norian) tetrapods from the southwestern United States. New Mexico Museum of Natural History and Science Bulletin 4:1–254.

Lucas, S. G. 2010. The Triassic timescale based on nonmarine tetrapod biostratigraphy and biochronology. Geological Society of London Special Publication 334:447–500.

Lucas, S. G., and A. B. Heckert. 1996a. Late Triassic aetosaur biochronology. Albertiana 17:57–64.

Lucas, S. G., and A. B. Heckert. 1996b. Vertebrate biochronology of the Late Triassic of Arizona; pp. 63–81 in D. Boaz, P. Dierking, R. Dornan, R. McGeorge, and B. J. Tegowski (eds.), Fossils of Arizona Volume 4, Proceedings of the Southwest Paleontological Society and Mesa Southwest Museum. Mesa Southwest Museum, Mesa, Arizona.

Lucas, S. G., J. A. Spielmann, and A. P. Hunt. 2007. Biochronological significance of Late Triassic tetrapods from Krasiejów, Poland. New Mexico Museum of Natural History and Science Bulletin 41:248–258.

Lydekker, R. 1894. Contributions to a knowledge of the fossil vertebrates of Argentina, Part II: the extinct edentates of Argentina. Anales del Museo de la Plata (Paleontologia Argentina) 3:1–118.

Maddison, W. P., and D. R. Maddison. 2018. Mesquite: a modular system for evolutionary analysis, version 3.51. Available at www.mesquiteproject.org. Accessed July 28, 2018.

Marsh, A. D., and T. B. Rowe. 2018. Anatomy and systematics of the sauropodomorph *Sarahsaurus aurifontanalis* from the Early Jurassic Kayenta Formation. PLoS One 13:e0204007.

Martz, J. W. 2002 The morphology and ontogeny of *Typothorax coccinarum* (Archosauria, Stagonolepididae) from the Upper Triassic of the American Southwest. M.Sc. thesis, Texas Tech University, Lubbock, Texas, 279 pp.

Martz, J. W., and W. G. Parker. 2010. Revised lithostratigraphy of the Sonsela Member (Chinle Formation, Upper Triassic) in the southern part of Petrified Forest National Park, Arizona. PLoS One 5:e9329.

Martz, J. W., and W. G. Parker. 2017. Revised formulation of the Late Triassic Land Vertebrate "Faunachrons" of western North America: recommendations for codifying nascent systems of vertebrate biochronology; pp. 39–124 in K. E. Zeigler and W. G. Parker (eds.), Terrestrial Depositional Systems: Deciphering Complexities Through Multiple Stratigraphic Methods. Elsevier, Amsterdam.

Martz, J. W., W. G. Parker, L. Skinner, J. J. Raucci, P. Umhoefer, and R. C. Blakey. 2012. Geologic map of Petrified Forest National Park, Arizona. Arizona Geological Survey Contributed Map CR-12-A, 1 map sheet, 1:50,000 map scale, 18 pp.

Martz, J. W., J. I. Kirkland, A. R. C. Milner, W. G. Parker, and V. L. Santucci. 2017. Upper Triassic lithostratigraphy, depositional systems, and vertebrate paleontology across southern Utah. Geology of the Intermountain West 4:99–180.

Mounce, R. C. P. 2013. Comparative cladistics: fossils, morphological data partitions and lost branches in the fossil tree of life. Ph.D. dissertation, The University of Bath, England, 161 pp.

Mukherjee, D. 2015. New insights from bone microanatomy of the Late Triassic *Hyperodapedon* (Archosauromorpha, Rhynchosauria): implications for archosauromorph growth strategy. Palaeontology 58:313–339.

Müller, R. T., M. B. von Baczko, J. B. Desojo, and S. J. Nesbitt. 2020. The first ornithosuchid from Brazil and its macroevolutionary and phylogenetic implications for Late Triassic faunas in Gondwana. Acta Palaeontologica Polonica 65. doi: 10.4202.app.00652.2019.

Murry, P. A. 1987. New reptiles from the Upper Triassic Chinle Formation of Arizona. Journal of Paleontology 61:773–786.

Murry, P. A., and R. A. Long. 1989. Geology and paleontology of the Chinle Formation, Petrified Forest National Park and vicinity, Arizona and a discussion of vertebrate fossils of the southwestern Upper Triassic; pp. 29–64 in S. G. Lucas and A. P. Hunt (eds.), Dawn of the Age of Dinosaurs in the American Southwest. New Mexico Museum of Natural History and Science, Albuquerque, New Mexico.

Nesbitt, S. J. 2005. Osteology of the Middle Triassic pseudosuchian archosaur *Arizonasaurus babbitti*. Historical Biology 17:19–47.

Nesbitt, S. J. 2007. The anatomy of *Effigia okeeffeae* (Archosauria, Suchia), theropod-like convergence, and the distribution of related taxa. Bulletin of the American Museum of Natural History 302:1–85.

Nesbitt, S. J. 2011. The early evolution of archosaurs: relationships and the origin of major clades. Bulletin of the American Museum of Natural History 352:1–292.

Nesbitt, S. J., and R. J. Butler. 2013a. Redescription of the archosaur *Parringtonia gracilis* from the Middle Triassic Manda beds of Tanzania, and the antiquity of Erpetosuchidae. Geological Magazine 150:225–238.

Nesbitt, S. J., and M. R. Stocker. 2008. The vertebrate assemblage of the Late Triassic Canjilon Quarry (northern New Mexico, USA), and the importance of apomorphy-based assemblage comparisons. Journal of Vertebrate Paleontology 28:1063–1072.

Nesbitt, S. J., R. B. Irmis, and W. G. Parker. 2007. A critical re-evaluation of the Late Triassic dinosaur taxa of North America. Journal of Systematic Palaeontology 5:209–243.

Nesbitt, S. J., J. Liu, and C. Li. 2011. A sail-backed suchian from the Heshanggou Formation (Early Triassic: Olenekian) of China. Earth and Environmental Science Transactions of the Royal Society of Edinburgh 101:271–284.

Nesbitt, S. J., A. H. Turner, and J. C. Weinbaum. 2013b. A survey of skeletal elements in the orbit of Pseudosuchia and the origin of the crocodylian palpebral. Earth and Environmental Science Transactions of the Royal Society of Edinburgh 103:365–607.

Nesbitt, S. J., M. R. Stocker, B. J. Small, and A. Downs. 2009. The osteology and relationships of *Vancleavea campi* (Reptilia: Archosauriformes). Zoological Journal of the Linnean Society 157:814–864.

Nesbitt, S. J., P. M. Barrett, S. Werning, C. A. Sidor, and A. J. Charig. 2012a. The oldest dinosaur? A Middle Triassic dinosauriform from Tanzania. Biology Letters 9:20120949.

Nesbitt, S. J., R. J. Butler, M. D. Ezcurra, A. J. Charig, and P. M. Barrett. 2018a. The anatomy of *Teleocrater rhadinus*, an early avemetatarsalian from the lower portion of the Lifua Member of the Manda Beds (Middle Triassic). Society of Vertebrate Paleontology Memoir 17:142–177.

Nesbitt, S. J., C. A. Sidor, K. D. Angielczyk, R. M. Smith, and W. G. Parker. 2012b. Derivation of the aetosaur osteoderm carapace: evidence from a new, exceptionally preserved "stem aetosaur" from

the Middle Triassic (Anisian) Manda Beds of southwestern Tanzania. Journal of Vertebrate Paleontology 32 (online supplement):149.

Nesbitt, S. J., C. A. Sidor, K. D. Angielczyk, R. M. Smith, and L. A. Tsuji. 2014. A new archosaur from the Manda Beds (Anisian, Middle Triassic) of southern Tanzania and its implications for character state optimizations at Archosauria and Pseudosuchia. Journal of Vertebrate Paleontology 34:1357–1382.

Nesbitt, S. J., J. J. Flynn, A. C. Pritchard, M. Parrish, L. Ranivoharimanana, and A. R. Wyss. 2015. Postcranial osteology of *Azendohsaurus madagaskarensis* (?Middle to Upper Triassic, Isalo Group, Madagascar) and its systematic position among stem archosaur reptiles. Bulletin of the American Museum of Natural History 398:1–126.

Nesbitt, S. J., C. A. Sidor, R. B. Irmis, K. D. Angielczyk, R. M. Smith, and L. A. Tsuji. 2010. Ecologically distinct dinosaurian sister group shows early diversification of Ornithodira. Nature 464:95–98.

Nesbitt, S. J., M. R. Stocker, W. G. Parker, T. A. Wood, C. A. Sidor, and K. D. Angielczyk. 2018b. The braincase and endocast of *Parringtonia gracilis*, a Middle Triassic suchian (Archosaur: Pseudosuchia). Society of Vertebrate Paleontology Memoir 17:122–141.

Nesbitt, S. J., R. J. Butler, M. D. Ezcurra, P. M. Barrett, M. R. Stocker, K. Angielcyyk, R. M. H. Smith, C. A. Sidor, G. Niedźwiedzki, A. G. Sennikov, and A. J. Charig. 2017. The earliest bird-line archosaurs and the assembly of the dinosaur body plan. Nature 544:484–487.

Norell, M. A., and W. Wheeler. 2003. Missing entry replacement data analysis: a replacement approach to dealing with missing data in paleontological and total evidence data sets. Journal of Vertebrate Paleontology 23:275–283.

Olsen, P. E., H.-D. Sues, and M. A. Norell. 2000. First record of *Erpetosuchus* (Reptilia: Archosauria) from the Late Triassic of North America. Journal of Vertebrate Paleontology 20:633–636.

Parker, W. G. 2005a. Faunal review of the Upper Triassic Chinle Formation of Arizona. Mesa Southwest Museum Bulletin 11:34–54.

Parker, W. G. 2005b. A new species of the Late Triassic aetosaur *Desmatosuchus* (Archosauria: Pseudosuchia). Comptes Rendu Paleovol 4:327–340.

Parker, W. G. 2007. Reassessment of the aetosaur '*Desmatosuchus*' *chamaensis* with a reanalysis of the phylogeny of the Aetosauria (Archosauria: Pseudosuchia). Journal of Systematic Paleontology 5:41–68.

Parker, W. G. 2008. Description of new material of the aetosaur *Desmatosuchus spurensis* (Archosauria: Suchia) from the Chinle Formation of Arizona and a revision of the genus *Desmatosuchus*. PaleoBios 28:1–40.

Parker, W. G. 2016a. Revised phylogenetic analysis of the Aetosauria (Archosauria: Pseudosuchia); assessing the effects of incongruent morphological character sets. PeerJ 4:e1583.

Parker, W. G. 2016b. Osteology of the Late Triassic archosaur *Scutarx deltatylus* (Archosauria: Pseudosuchia). PeerJ 4:e2411.

Parker, W. G. 2018a. Redescription of *Calyptosuchus* (*Stagonolepis*) *wellesi* (Archosauria: Pseudosuchia: Aetosauria) from the Late Triassic of the Southwestern United States with a discussion of genera in vertebrate paleontology. PeerJ 6:e4291.

Parker, W. G. 2018b. Anatomical notes and discussion of the first described aetosaur *Stagonolepis robertsoni* (Archosauria: Suchia) from the Upper Triassic of Europe, and the use of plesiomorphies in aetosaur biochronology. PeerJ 6:e5455.

Parker, W. G., and B. J. Barton. 2008. New information on the Upper Triassic archosauriform *Vancleavea campi* based on new material from the Chinle Formation of Arizona. Palaeontologia Electronica 11:1–20.

Parker, W. G., and J. W. Martz. 2011. The Late Triassic (Norian) Adamanian-Revueltian tetrapod faunal transition in the Chinle Formation of Petrified Forest National Park, Arizona. Earth and Environmental Science Transactions of the Royal Society of Edinburgh 101:231–260.

Parker, W. G., M. R. Stocker, and R. B. Irmis. 2008. A new desmatosuchine archosaur (Archosauria: Pseudosuchia) from the Upper Triassic Tecovas Formation (Dockum Group) of Texas. Journal of Vertebrate Paleontology 28:692–701.

Parker, W. G., R. B. Irmis, S. J. Nesbitt, J. W. Martz, and L. S. Browne. 2005. The Late Triassic pseudosuchian *Revueltosaurus callenderi* and its implications for the diversity of early ornithischian dinosaurs. Proceedings of the Royal Society of London, Biological Sciences 272:963–969.

Parrish, J. M. 1993. Phylogeny of the Crocodylotarsi, with reference to archosaurian and crurotarsan monophyly. Journal of Vertebrate Paleontology 13:287–308.

Parrish, J. M. 1994. Cranial osteology of *Longosuchus meadei* and the phylogeny and distribution of the Aetosauria. Journal of Vertebrate Paleontology 14:196–209.

Parrish, J. M. 1999. Small fossil vertebrates from the Chinle Formation (Upper Triassic) of southern Utah. Utah Geological Survey Miscellaneous Publication 99-1:45–50.

Parrish, J. M., and S. C. Good. 1987. Preliminary report on vertebrate and invertebrate fossil occurrences, Chinle Formation (Upper Triassic), southeastern Utah. Four Corners Geological Society Guidebook 10:109–115.

Pinheiro, F. L., M. A. G. França, M. B. Lacerda, R. J. Butler, and C. L. Schultz. 2016. An exceptional fossil skull from South America and the origins of the archosauriform radiation. Scientific Reports 6:22817.

Polcyn, M. J., D. A. Winkler, L. L. Jacobs, and K. Newman. 2002. Fossil occurrences and structural disturbance in the Triassic Chinle Formaton at North Stinking Springs Mountain near St. Johns, Arizona. New Mexico Museum of Natural History and Science Bulletin 21:43–50.

Pritchard, A. C., and H.-D. Sues. 2019. Postcranial remains of *Teraterpeton hrynewichorum* (Reptilia: Archosauromorpha) and the mosaic evolution of the saurian postcranial skeleton. Journal of Systematic Palaeontology 17:1745–1765.

Pritchard, A. C., A. H. Turner, S. J. Nesbitt, R. B. Irmis, and N. D. Smith. 2015. Late Triassic tanystropheids (Reptilia, Archosauromorpha) from northern New Mexico (Petrified Forest Member, Chinle Formation) and the biogeography, functional morphology, and evolution of Tanystropheidae. Journal of Vertebrate Paleontology 35:e911186.

Pritchard, A. C., J. A. Gauthier, M. Hanson, G. S. Bever, and B.-A. S. Bhullar. 2018. A tiny Triassic saurian from Connecticut and the early evolution of the diapsid feeding apparatus. Nature Communications 9:1213.

Rae, T. C. 1999. Mosaic evolution in the origin of Hominoidea. Folia Primatologia 70:125–135.

Ramezani, J., G. D. Hoke, D. E. Fastovsky, S. A. Bowring, F. Therrien, S. T. Dworkin, S. C. Atchley, and L. C. Nordt. 2011. High-precision U-Pb zircon geochronology of the Late Triassic Chinle Formation, Petrified Forest National Park (Arizona, USA): temporal constraints on the early evolution of dinosaurs. Geological Society of America Bulletin 123:2142–2159.

Ramezani, J., D. E. Fastovsky, and S. A. Bowring. 2014. Revised chronostratigraphy of the lower Chinle Formation strata in Arizona and New Mexico (USA): high-precision U-Pb geochronological constraints on the Late Triassic evolution of dinosaurs. American Journal of Science 314:981–1008.

Ray, S., and A. Chinsamy. 2004. *Diictodon feliceps* (Therapsida, Dicynodontia): bone histology, growth, and biomechanics. Journal of Vertebrate Paleontology 24:180–194.

Reyes, W. A., W. G. Parker, and A. D. Marsh. In review. Cranial anatomy and dentition of the aetosaur *Typothorax coccinarum* (Archosauria: Pseudosuchia) from the Upper Triassic Chinle Formation. Journal of Vertebrate Paleontology.

Sawin, H. J. 1947. The pseudosuchian reptile *Typothorax meadei*. Journal of Paleontology 21:231–238.

Scheyer, T. M., J. B. Desojo, and I. A. Cerda. 2014. Bone histology of phytosaur, aetosaur, and other archosauriform osteoderms (Eureptilia, Archosauromorpha). Anatomical Record 297:240–260.

Scheyer, T. M., and H.-D. Sues. 2016. Expanded dorsal ribs in the Late Triassic pseudosuchian reptile *Euscolosuchus olseni*. Journal of Vertebrate Paleontology 37:e1248768.

Schoch, R. R. 2007. Osteology of the small archosaur *Aetosaurus* from the Upper Triassic of Germany. Neues Jahrbuch für Geologie und Paläontologie Abhandlungen 246:1–35.

Schoch, R. R., and J. Desojo. 2016. Cranial anatomy of the aetosaur *Paratypothorax andressorum* Long and Ballew, 1985, from the Upper Triassic of Germany and its bearing on aetosaur phylogeny. Neues Jahrbuch für Geologie und Paläontologie Abhandlungen 279:73–95.

Sengupta, S., M. D. Ezcurra, and S. Bandyopadhyay. 2017. A new horned and long-necked herbivorous stem-archosaur from the Middle Triassic of India. Nature Scientific Reports 7:8366.

Sereno, P. C. 1991. Basal archosaurs: phylogenetic relationships and functional implications. Society of Vertebrate Paleontology Memoir 2:1–53.
Sereno, P. C. 2005. The logical basis of phylogenetic taxonomy. Systematic Biology 54:595–619.
Small, B. J. 1985 The Triassic thecodontian reptile *Desmatosuchus*: osteology and relationships. M.Sc. thesis, Texas Tech University, Lubbock, Texas, 83 pp.
Small, B. J. 2002. Cranial anatomy of *Desmatosuchus haplocerus* (Reptilia: Archosauria: Stagonolepididae). Zoological Journal of the Linnean Society 136:97–111.
Small, B. J., and J. W. Martz. 2013. A new aetosaur from the Upper Triassic Chinle Formation of the Eagle Basin, Colorado, USA. Geological Society Special Publication 379:393–412.
Sookias, R. B. 2016. The relationships of the Euparkeriidae and the rise of Archosauria. Royal Society Open Science 3:150674.
Stefanic, C. M., and S. J. Nesbitt. 2019. The evolution and role of hyposphene-hypantrum articulation in Archosauria: phylogeny, size and/or mechanics? Royal Society Open Science 6:190258.
Sterli, J., and M. S. de la Fuente. 2011. Re-description and evolutionary remarks on the Patagonian horned turtle *Niolamia argentina* Ameghino, 1899 (Testudinata, Meiolaniidae). Journal of Vertebrate Paleontology 31:1210–1229.
Stocker, M. R. 2010. A new taxon of phytosaur (Archosauria: Pseudosuchia) from the Late Triassic (Norian) Sonsela Member (Chinle Formation) in Arizona, and a critical reevaluation of *Leptosuchus* Case 1922. Palaeontology 53:997–1022.
Stocker, M. R., S. J. Nesbitt, K. E. Criswell, W. G. Parker, L. M. Witmer, T. B. Rowe, R. Ridgely, and M. A. Brown. 2016. A dome-headed stem archosaur exemplifies convergence among dinosaurs and their distant relatives. Current Biology 26:1–7.
Sues, H.-D. 1992. A remarkable new armored archosaur from the Upper Triassic of Virginia. Journal of Vertebrate Paleontology 12:142–149.
Sues, H.-D. 2003. An unusual new archosauromorph reptile from the Upper Triassic Wolfville Formation of Nova Scotia. Canadian Journal of Earth Sciences 40:635–649.
Taborda, J. R. A., I. A. Cerda, and J. B. Desojo. 2013. Growth curve of *Aetosauroides scagliai* Casamiquela 1960 (Pseudosuchia: Aetosauria) inferred from osteoderm histology. Geological Society of London Special Publication 379:413–423.
Takhtajan, A. 1991. Evolutionary Trends in Flowering Plants. Cambridge University Press, Cambridge, U.K., 268 pp.
Thompson, D. W. 1917. On Growth and Form. Cambridge University Press, Cambridge, U.K., 793 pp.
Tsai, C.-H., and R. E. Fordyce. 2014. Juvenile morphology in baleen whale phylogeny. Naturwissenschaften 101:765–769.
Tucker, A. D. 1997. Validation of skeletochronology to determine age of freshwater crocodiles (*Crocodylus johnstoni*). Marine & Freshwater Research 48:343–351.
Tykoski, R. S. 2005. Anatomy, ontogeny, and phylogeny of coelophysoid theropods. Ph.D. dissertation, University of Texas at Austin, Austin, Texas, 553 pp.
Wall, W. P. 1983. The correlation between high limb-bone density and aquatic habits in Recent mammals. Journal of Paleontology 57:197–207.
Walker, A. D. 1961. Triassic reptiles from the Elgin area: *Stagonolepis*, *Dasygnathus* and their allies. Philosophical Transactions of the Royal Society of London, Series B 244:103–204.
Walker, A. D. 1964. Triassic reptiles from the Elgin area: *Ornithosuchus* and the origin of carnosaurs. Philosophical Transactions of the Royal Society of London, Series B 248:53–134.
Wiens, J. J., R. M. Bonett, and P. T. Chippindale. 2005. Ontogeny discombobulates phylogeny: paedomorphosis and higher-level salamander relationships. Systematic Biology 54:91–110.
Wilson, J. A. 1999. A nomenclature for vertebral laminae in sauropods and other saurischian dinosaurs. Journal of Vertebrate Paleontology 19:639–653.
Wilson, J. A., M. D. D'Emic, T. Ikejiri, E. M. Moacdieh, and J. A. Whitlock. 2011. A nomenclature for vertebral fossae in sauropods and other saurischian dinosaurs. PLoS One 6:e17144.
Woodward, A. R., and C. T. Moore. 1992. *Alligator* age determination. Florida Game and Fresh Water Fish Commission Bureau of Wildlife Research Final Report 7563:1–20.
Woody, D. T. 2003. Revised geological assessment of the Sonsela Member, Chinle Formation, Petrified Forest National Park, Arizona. M.Sc. thesis, Northern Arizona University, Flagstaff, Arizona, 206 pp.
Wynd, B. M., S. J. Nesbitt, M. R. Stocker, and A. B. Heckert. 2020. A detailed description of *Rugarhynchos sixmilensis*, gen. et comb. nov. (Archosauriformes, Proterochampsia), and cranial convergence in snout elongation across stem and crown archosaurs. Journal of Vertebrate Paleontology 39:e1748042.
Zittel, K. A. von. 1887. Handbuch der Paläontologie. 1. Abteilung: Paläozoologie, Band 3, Vertebrata (Pisces, Amphibia, Reptilia, Aves). Druck und Verlag von R. Oldenbourg, München, 900 pp.
Zurita, A. E., L. R. González Ruiz, A. J. Gómez-Cruz, and J. E. Arenas-Mosquera. 2013. The most complete known Neogene Glyptodontidae (Mammalia, Xenarthra, Cingulata) from northern South America: taxonomic, paleobiogeographic, and phylogenetic implications. Journal of Vertebrate Paleontology 33:696–708.

Submitted March 13, 2020; revisions received May 29, 2020;
accepted June 3, 2020.
Handling Editor: Lindsay Zanno.

APPENDIX 1. List of referred specimens of *Acaenasuchus geoffreyi* Long and Murry, 1995.

Maxilla—PEFO 43699.
Frontal—PEFO 44457, UCMP 285854.
Parietal—UCMP 285909.
Jugal—UCMP 285909.
Squamosal—UCMP 285837.
Articular and Surangular—MNA V3679, UCMP 293853.
Cranial Fragment—PEFO 40711, UCMP 285903.
Vertebra—PEFO 38748, PEFO 40693, PEFO 40687, PEFO 40703, PEFO 40706, PEFO 40712, PEFO 40723, PEFO 40731, PEFO 40738, MNA V2877, UCMP 192558, UCMP 195222, UCMP 285836, UCMP 285856, UCMP 285858, UCMP 285875, UCMP 285904, UMNH VP 30183.
Rib—EFO 40703, PEFO 40712, PEFO 40721, PEFO 40723, PEFO 40738, UCMP 285842.
Scapula—PEFO 40720, UCMP 285840.
Coracoid—UCMP 285851.
Humerus—PEFO 40693, PEFO 40704, PEFO 40739.
Ulna—UCMP 285835.
Ilium—PEFO 16638, PEFO 40720, PEFO 40731, UCMP 285833, UCMP 285909.
Pubis—PEFO 40693, UCMP 285841, UCMP 285851.
Ischium—PEFO 40693.
Femur—PEFO 38762, PEFO 38763, PEFO 40696, PEFO 40720, PEFO 40734, MNA V3048.
Tibia—PEFO 40731.
Articulated Osteoderm—PEFO 38737, PEFO 40702, PEFO 40740, PEFO 44449, MNA V3043, MNA V3066, UCMP 139582, UCMP 175109, UCMP 175111.
Paramedian Osteoderm—PEFO 16621, PEFO 37181, PEFO 37185, PEFO 37223, PEFO 37326, PEFO 38363, PEFO 40000, PEFO 40694, PEFO 40706, PEFO 40742, PEFO 44448, PEFO 44450, PEFO 44452, PEFO 44455, MNA V3040, MNA V3067, MNA V3113, MNA V3632, MNA V3668, MNA V3714, UMNH VP 30185, UMNH VP 30186, UMNH VP 30208, UMNH VP 30209, UMNH VP 30210, UMNH VP 30217, UCMP 139576 (holotype), UCMP 139586, UCMP 139587, UCMP 139588, UCMP 156046, UCMP 165214, UCMP 175068, UCMP 175073, UCMP 175082, UCMP 175084, UCMP 175085, UCMP 175093, UCMP 175100, UCMP 175101, UCMP 175102, UCMP 175103, UCMP 175105, UCMP 175121, UCMP 175132, UCMP 175133, UCMP 175138, UCMP 195236, UCMP 195240, UCMP 195248, UCMP 285847, UCMP 285848, UCMP 285865, UCMP 285867, UCMP 285868, UCMP 285872, UCMP 285878, UCMP 285888, UCMP 285889, UCMP 285901, UCMP 285905, UCMP 30185, UCMP 30186, UCMP 30208, UCMP 30209, UCMP 30210, UCMP 30217.

Lateral Osteoderm—PEFO 37181, PEFO 37245, PEFO 38744, PEFO 38774, PEFO 40741, PEFO 44451, PEFO 44453, PEFO 44454, PEFO 44456, MNA V3046, MNA V3631, UMNH VP 30184, UCMP 139577, UCMP 139578, UCMP 139579, UCMP 139580, UCMP 139581, UCMP 139583, UCMP 139589, UCMP 139590, UCMP 139591, UCMP 139592, UCMP 139593, UCMP 139594, UCMP 139595, UCMP 139596, UCMP 139597, UCMP 139598, UCMP 139599, UCMP 139600, UCMP 139601, UCMP 139603, UCMP 139604, UCMP 139605, UCMP 139606, UCMP 139607, UCMP 139608, UCMP 139609, UCMP 139611, UCMP 139612, UCMP 139614, UCMP 139615, UCMP 139616, UCMP 139617, UCMP 139618, UCMP 139619, UCMP 139621, UCMP 156046, UCMP 175096, UCMP 175106, UCMP 175107, UCMP 175108, UCMP 175110, UCMP 175113, UCMP 175114, UCMP 175115, UCMP 175116, UCMP 175117, UCMP 175118, UCMP 175119, UCMP 175120, UCMP 175123, UCMP 175124, UCMP 175125, UCMP 175126, UCMP 195232, UCMP 195233, UCMP 195234, UCMP 195235, UCMP 195237, UCMP 195238, UCMP 195243, UCMP 195244, UCMP 195245, UCMP 195246, UCMP 195247, UCMP 285831, UCMP 285849, UCMP 285855, UCMP 285857, UCMP 285863, UCMP 285871, UCMP 285874, UCMP 285877, UCMP 285887, UCMP 285934.

Ventral Osteoderm—UCMP 139602, UCMP 139610, UCMP 139620, UCMP 175060, UCMP 175069, UCMP 175074, UCMP 175081, UCMP 175097, UCMP 175134, UCMP 175135, UCMP 175139, UCMP 195241, UCMP 285829, UCMP 285834, UCMP 285861, UCMP 285879, UCMP 285881, UCMP 285883, UCMP 285864.

Partial Osteoderm—PEFO 20358, PEFO 37171, PEFO 37173, PEFO 37181, PEFO 37233, PEFO 37245, PEFO 37323, PEFO 37326, PEFO 38264, PEFO 38738, PEFO 38761, PEFO 40692, PEFO 40701, PEFO 40713, PEFO 40721, PEFO 40722, PEFO 40732, PEFO 40734, PEFO 40736, PEFO 40744, PEFO 40747, PEFO 40748, PEFO 40749, PEFO 40750, PEFO 40751, MNA V2921, MNA V2952, MNA V3002, MNA V3007, MNA V3050, MNA V3679, UCMP 139613, UCMP 175071, UCMP 175122, UCMP 175127, UCMP 175128, UCMP 175129, UCMP 175141, UCMP 175155, UCMP 195239, UCMP 195242, UCMP 285839, UCMP 285845, UCMP 285846, UCMP 285850, UCMP 285852, UCMP 285853, UCMP 285859, UCMP 285860, UCMP 285862, UCMP 285873, UCMP 285876, UCMP 285882, UCMP 285884, UCMP 285885, UCMP 285886, UCMP 285890, UCMP 285891, UCMP 285892, UCMP 285899, UCMP 285902, UCMP 285907, UCMP 285908, UCMP 285910, UCMP 139586 (139584 label), UCMP 139586 (139585 label), UCMP 139586 (139586 label), UCMP 175130 (175130 label), UCMP 175130 (175131 label), UCM 76194.